



Since January 2020 Elsevier has created a COVID-19 resource centre with free information in English and Mandarin on the novel coronavirus COVID-19. The COVID-19 resource centre is hosted on Elsevier Connect, the company's public news and information website.

Elsevier hereby grants permission to make all its COVID-19-related research that is available on the COVID-19 resource centre - including this research content - immediately available in PubMed Central and other publicly funded repositories, such as the WHO COVID database with rights for unrestricted research re-use and analyses in any form or by any means with acknowledgement of the original source. These permissions are granted for free by Elsevier for as long as the COVID-19 resource centre remains active.



## Synthesis and characterization of 1,2,4-triazolo[1,5-*a*]pyrimidine-2-carboxamide-based compounds targeting the PA-PB1 interface of influenza A virus polymerase



Serena Massari <sup>a,\*</sup>, Chiara Bertagnin <sup>b</sup>, Maria Chiara Pismataro <sup>a</sup>, Anna Donnadio <sup>a</sup>, Giulio Nannetti <sup>b</sup>, Tommaso Felicetti <sup>a</sup>, Stefano Di Bona <sup>c</sup>, Maria Giulia Nizi <sup>a</sup>, Leonardo Tensi <sup>c</sup>, Giuseppe Manfroni <sup>a</sup>, Maria Isabel Loza <sup>d</sup>, Stefano Sabatini <sup>a</sup>, Violetta Cecchetti <sup>a</sup>, Jose Brea <sup>d</sup>, Laura Goracci <sup>c</sup>, Arianna Loregian <sup>b,1</sup>, Oriana Tabarrini <sup>a,1</sup>

<sup>a</sup> Department of Pharmaceutical Sciences, University of Perugia, 06123, Perugia, Italy

<sup>b</sup> Department of Molecular Medicine, University of Padua, 35121, Padua, Italy

<sup>c</sup> Department of Chemistry, Biology and Biotechnology, University of Perugia, 06123, Perugia, Italy

<sup>d</sup> CIMUS Research Center, University of Santiago de Compostela, 15782, Santiago de Compostela, Spain

### ARTICLE INFO

#### Article history:

Received 13 September 2020

Received in revised form

13 October 2020

Accepted 13 October 2020

#### Keywords:

Influenza virus

PA-PB1 heterodimerization

RNA-Dependent RNA polymerase

Protein-protein interaction

### ABSTRACT

Influenza viruses (Flu) are responsible for seasonal epidemics causing high rates of morbidity, which can dramatically increase during severe pandemic outbreaks. Antiviral drugs are an indispensable weapon to treat infected people and reduce the impact on human health, nevertheless anti-Flu armamentarium still remains inadequate.

In search for new anti-Flu drugs, our group has focused on viral RNA-dependent RNA polymerase (RdRP) developing disruptors of PA-PB1 subunits interface with the best compounds characterized by cycloheptathiophene-3-carboxamide and 1,2,4-triazolo[1,5-*a*]pyrimidine-2-carboxamide scaffolds. By merging these moieties, two very interesting hybrid compounds were recently identified, starting from which, in this paper, a series of analogues were designed and synthesized. In particular, a thorough exploration of the cycloheptathiophene-3-carboxamide moiety led to acquire important SAR insight and identify new active compounds showing both the ability to inhibit PA-PB1 interaction and viral replication in the micromolar range and at non-toxic concentrations. For few compounds, the ability to efficiently inhibit PA-PB1 subunits interaction did not translate into anti-Flu activity. Chemical/physical properties were investigated for a couple of compounds suggesting that the low solubility of compound **14**, due to a strong crystal lattice, may have impaired its antiviral activity. Finally, computational studies performed on compound **23**, in which the phenyl ring suitably replaced the cycloheptathiophene, suggested that, in addition to hydrophobic interactions, H-bonds enhanced its binding within the PA<sub>C</sub> cavity.

© 2020 Elsevier Masson SAS. All rights reserved.

### 1. Introduction

Influenza (Flu) viruses are responsible for seasonal epidemics resulting in about 3–5 million cases of severe respiratory illness and 290,000 to 650,000 deaths each year all over the world [1]. Moreover, they are also able to generate pandemic outbreaks that occur when new highly virulent FluA subtypes generated by

antigenic shift are transmitted from animals to humans and sustainably spread among people.

In 1918, humanity experienced the “Spanish Flu” caused by FluA (H1N1) [2], an influenza pandemic that intensively and speedily struck world population infecting about 500 million people and killing from 20 to 40 million people globally [3]. Other two pandemics occurred in 20th century: the “Asian Flu” caused by Flu A (H2N2) virus [4], which started in China in 1957 and spread globally causing about one to four million deaths, and the “1968 Flu pandemic” caused by Flu A (H3N2) virus, which started in Hong Kong and spread to the United States causing one million deaths. In 2003, the avian Flu A (H5N1) re-emerged passing the species

\* Corresponding author.

E-mail address: [serena.massari@unipg.it](mailto:serena.massari@unipg.it) (S. Massari).

<sup>1</sup> Co-last authors.

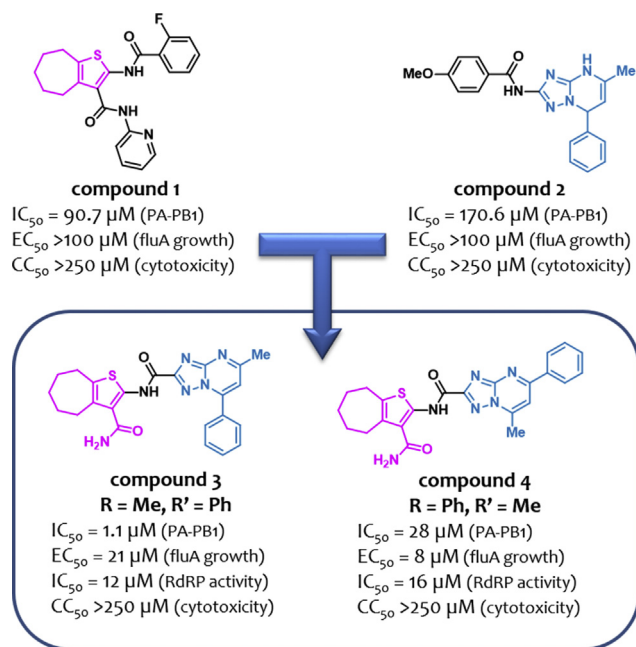


**Fig. 1.** Structures and biological activities of compounds 1–4 previously reported [27,32].

barrier but fortunately not spreading sustainably from person to person, while, in 2009, the “swine Flu” A (H1N1) virus was responsible for the first pandemic of the 21st century [5]; it started in Mexico and spread rapidly around the world causing from 150,000 to 600,000 deaths [6]. To date, the avian Flu A (H5N1) and

Flu A (H7N9) are of particular concern to public health due to their potential to cause an influenza pandemic [7].

Previous pandemic events from Flu viruses highlighted that a vaccine is an essential mean to rapidly prevent the spread of infection, but, in the absence of a vaccine, antiviral drugs could be a valid weapon to treat infected people and reduce the impact on human health. Unfortunately, a universal anti-Flu vaccine does not exist yet, so in case of a pandemic event, a new specific vaccine should be developed on the basis of the emerging strain.

Regarding the anti-flu treatment, until recently, the only approved anti-Flu drugs were the NA inhibitors oseltamivir and zanamivir (laninamivir octanoate and peramivir were approved only in some Asian countries), and adamantanes targeting the M2 ion channels protein, although the latter are no longer recommended due to the emergence of widespread resistance [8]. This limited therapeutic armamentarium was recently enriched by a new class of anti-Flu drugs involved in the inhibition of the RNA-dependent RNA polymerase (RdRP) [9–12]. In particular, the nucleoside analog favipiravir was approved in 2014 in Japan for stockpiling against Flu pandemics [13]; to date, the safety and efficacy of favipiravir are also being evaluated in seven clinical trials against COVID-19. In 2018, the endonuclease inhibitor baloxavir marboxil was approved in both Japan and the United States [14]; moreover, the cap-binding inhibitor pimodivir is currently in late phase clinical trials [15].

The RdRP is thus emerging as an important drug-target [16–18]. It is a heterotrimer composed by the polymerase basic protein 1 (PB1), polymerase basic protein 2 (PB2), and polymerase acidic protein (PA, P3 in FluC) subunits. The three RdRP subunits are connected in head-to-tail fashion by extensive interactions that occur between the PB1<sub>N</sub> and PA<sub>C</sub> termini and the PB1<sub>C</sub> and PB2<sub>N</sub> termini. In the context of the viral ribonucleoprotein complex

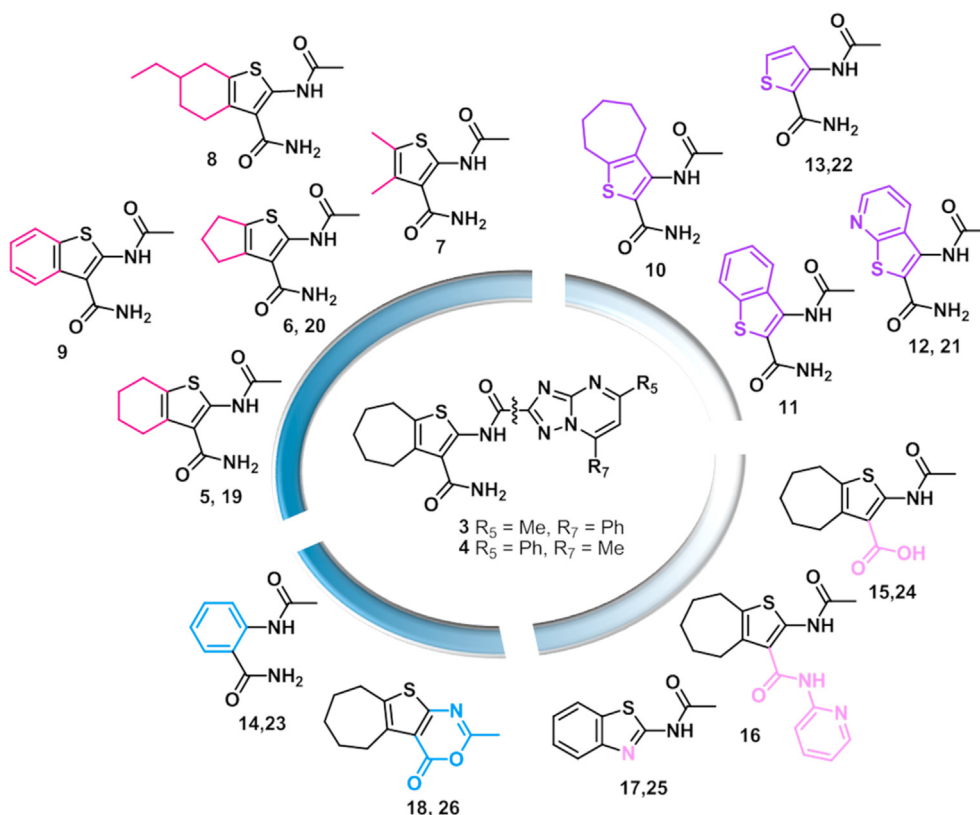


**Fig. 2.** Structure of the compounds synthesized in this study. Compounds 5–18 are analogues of compound 3 and compounds 19–26 are analogues of compound 4.

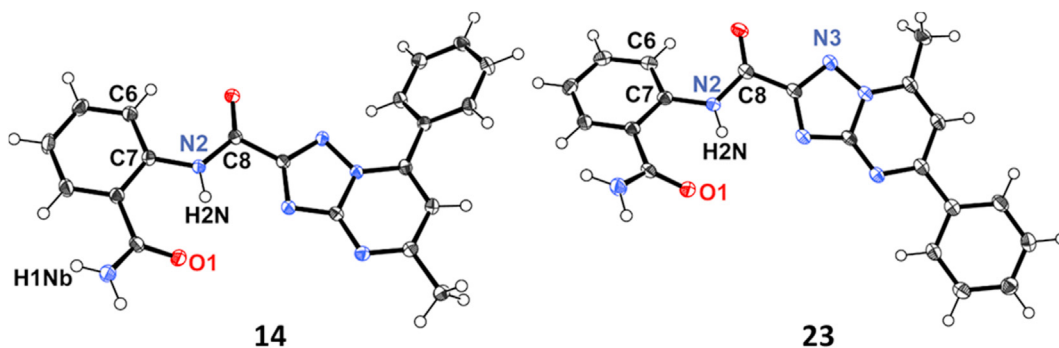


Fig. 3. Asymmetric unit of **14** and **23**, showing a partial atom-numbering scheme. Displacement ellipsoids are drawn at 50% probability level.

(vRNP), the RdRP plays a key role in the viral life cycle performing both the transcription and replication of viral genome [19,20].

The publication of crystal structures of PA<sub>C</sub>-PB1<sub>N</sub> interface (pdb codes: 3CM8 [21] and 2ZNL [22]) prompted the search for small-molecule inhibitors of this protein-protein interaction (PPI) able

to interfere with RdRP functions [23–25]. We have been pioneers in this research field, identifying several compounds characterized by different chemotypes. In particular, with the exception of compound AL18 that was found serendipitously [26], all the other PA-PB1 inhibitors have been identified by an initial structure-based

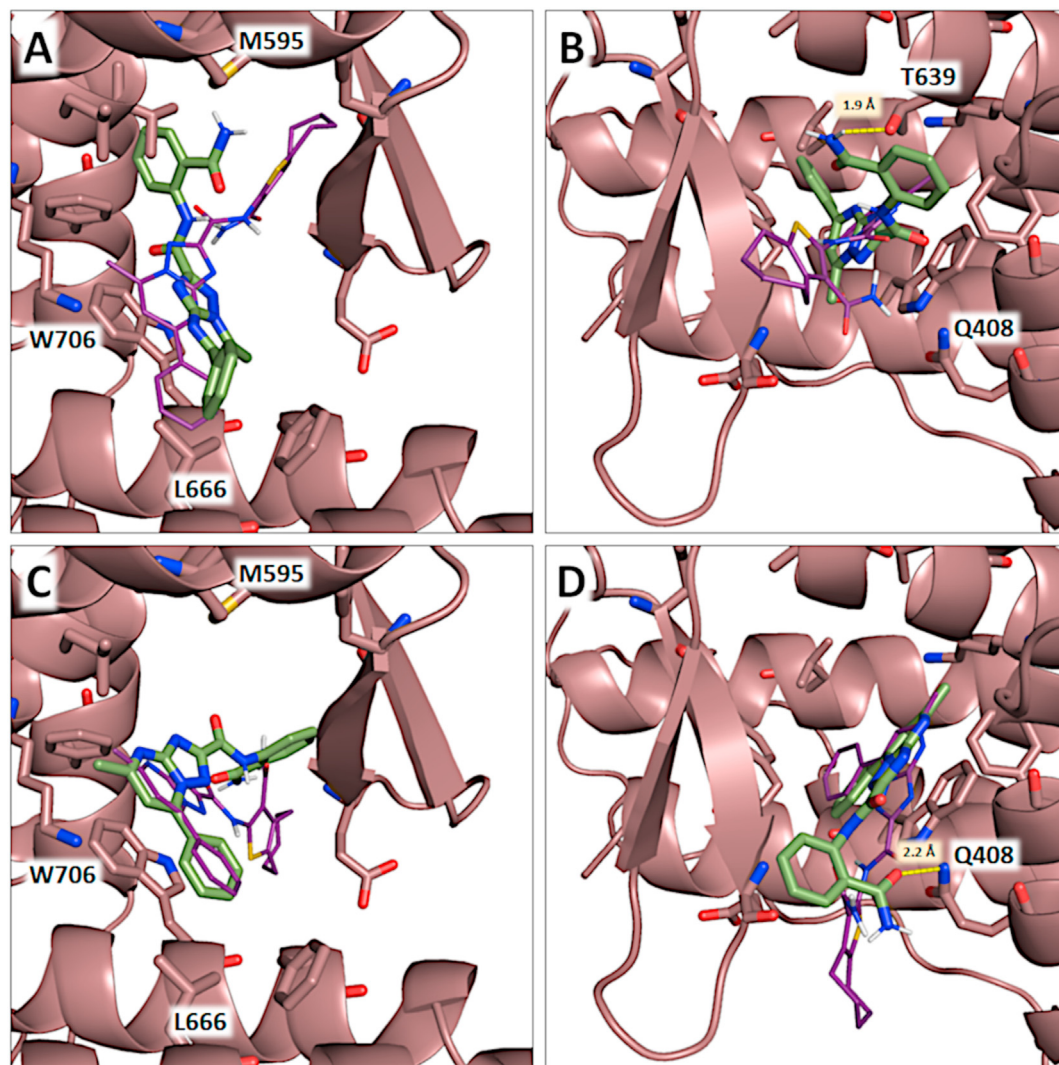
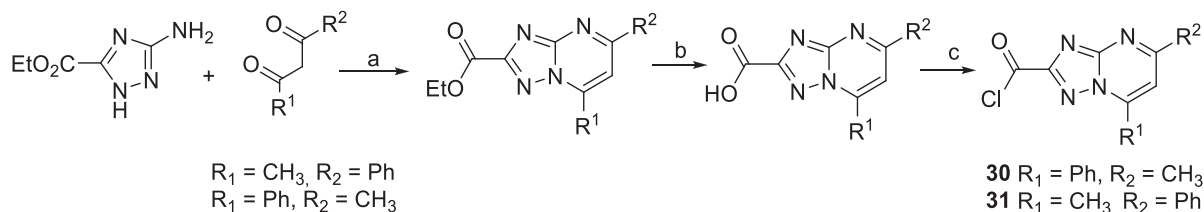


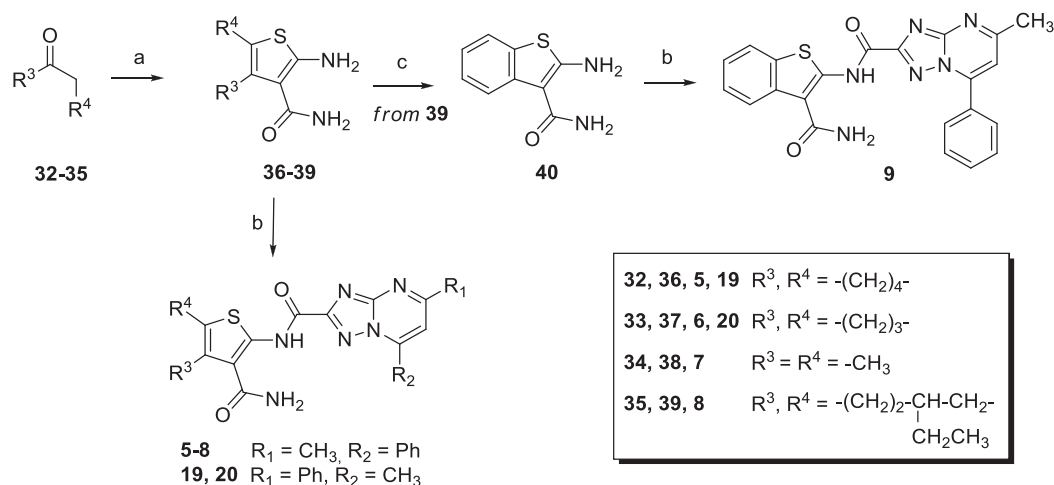
Fig. 4. FLAP binding poses for compounds **23** (A,B) and **14** (C,D). Two orientations of the same pose in the PA cavity are illustrated to better visualize the predicted interactions. Compounds **14** and **23** are shown in sticks mode and in green color, while reference compounds **3** and **4** are shown in lines style and purple color. (For interpretation of the references to color in this figure legend, the reader is referred to the Web version of this article.)



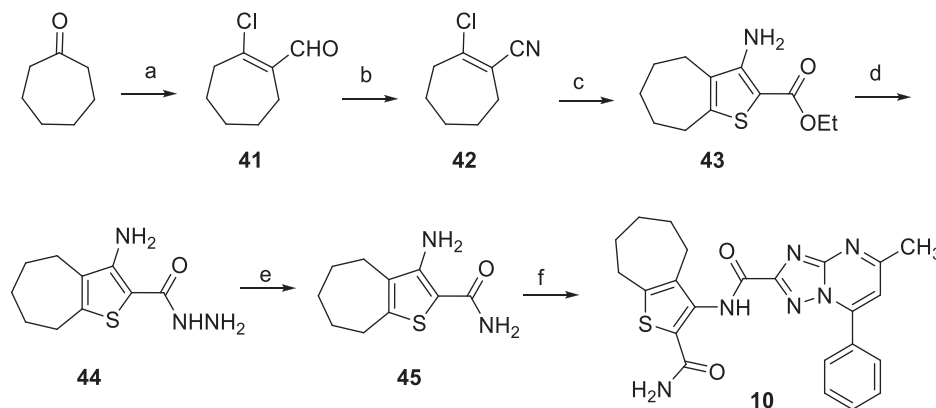
**Scheme 1.** Synthetic route of the intermediates **30** and **31**. Reagents and conditions: (a) glacial acetic acid, reflux; (b) NaOH, MeOH, reflux; (c) oxalyl chloride,  $\text{CH}_2\text{Cl}_2$ , DMF, room temperature (r.t.).

drug design [27,28] followed by hit-to-lead optimization campaigns, such as cycloheptathiophene-3-carboxamide (cHTC) [29–31], 1,2,4-triazolo[1,5-*a*]pyrimidine (TZP) [32], pyrazolo[1,5-*a*]pyrimidine [33] and 3-cyano-4,6-diphenylpyridine [34] derivatives. During the optimization of cHTC derivative **1** [27] and TZP derivative **2** [27] (Fig. 1), hybrid compounds **3** and **4** (Fig. 1) were prepared by joining the cHTC and the TZP moieties, exhibiting very interesting activities [32]. In particular, compound **3**, with an  $\text{IC}_{50} = 1.1 \mu\text{M}$ , emerged as one of the most potent among the small-molecule PA-PB1 inhibitors developed so far.

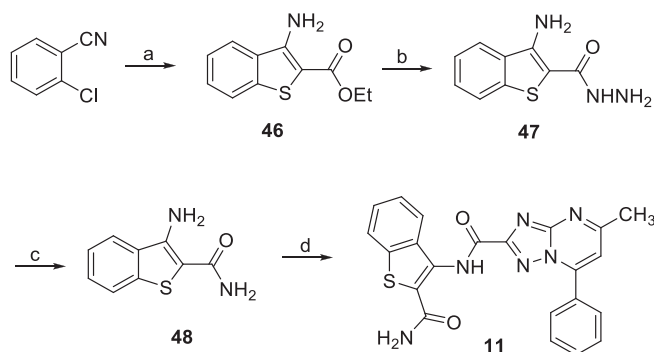
Accordingly, it affected PA-PB1 binding in the cell cytoplasm and blocked the intranuclear translocation of PA, which requires the formation of the PA-PB1 complex. Compound **3** also showed good anti-polymerase activity ( $\text{IC}_{50} = 12 \mu\text{M}$  in minireplicon assay) and broad anti-FluA and -FluB activity ( $\text{EC}_{50}$ s ranging from 7 to 25  $\mu\text{M}$ , in MDCK cells) without showing any cytotoxicity up to concentrations of 250  $\mu\text{M}$ . Compound **4** exhibited slightly better antiviral activity ( $\text{EC}_{50}$  values ranging from 5 to 14  $\mu\text{M}$  against FluA and FluB strains), even if it was endowed with lower ability to inhibit the PA-PB1 interaction ( $\text{IC}_{50} = 28 \mu\text{M}$ ) [32].



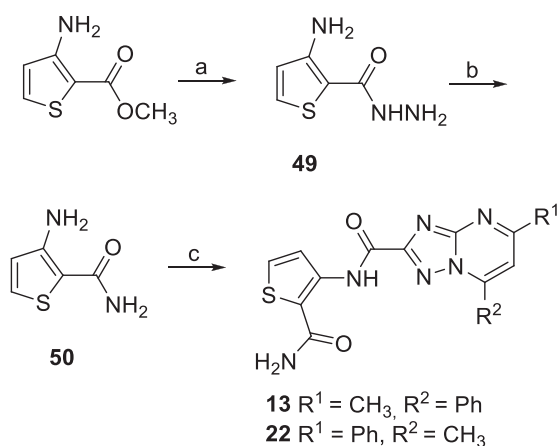
**Scheme 2.** Synthetic route of the target compounds **5–8, 19** and **20**. Reagents and conditions: (a) sulphur, *N,N*-diethylamine, EtOH, rt or sulphur, morpholine, EtOH, reflux; (b) compound **30** or **31**,  $\text{CH}_2\text{Cl}_2$ , DIPEA, rt; (c) *p*-chloranil, 1,4-dioxane, 90 °C.



**Scheme 3.** Synthetic route of the target compound **10**. Reagents and conditions: (a) DMF,  $\text{POCl}_3$ , from 0 °C to r. t.; (b) NMP,  $\text{NH}_2\text{OH}$  hydrochloride, 115 °C; (c)  $\text{K}_2\text{CO}_3$ , MeOH/THF (5:1), ethyl thioglycolate, reflux; (d)  $\text{NH}_2\text{NH}_2$  hydrate, 80 °C; (e) Ni-Raney, DMF, 90 °C; (f) compound **30**,  $\text{CH}_2\text{Cl}_2$ , DIPEA, rt.

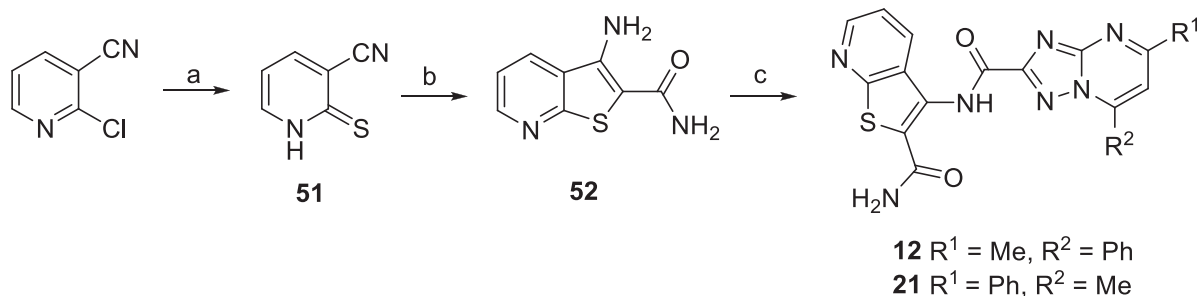


**Scheme 4.** Synthetic route of the target compound **11**. Reagents and conditions: (a) ethyl thioglycolate, DMF, KOH, from 0 °C to 80 °C; (b)  $\text{NH}_2\text{NH}_2$  hydrate, 80 °C; (c) Ni-Raney, DMF, 90 °C; (d) compound **30**,  $\text{CH}_2\text{Cl}_2$ , DIPEA, rt.



**Scheme 5.** Synthetic route of the target compounds **13** and **22**. Reagents and conditions: (a)  $\text{NH}_2\text{NH}_2$  hydrate, 80 °C; (b) Ni-Raney, DMF, 90 °C; (c) compound **30** or **31**,  $\text{CH}_2\text{Cl}_2$ , DIPEA, rt.

Computational studies performed on the positional isomers **3** and **4** within the  $\text{PA}_C$  cavity suggested that the molecules have a different orientation and extents of hydrophobic and H-bond interactions within the cavity [32]. Thus, while the elongated shape of **4** allows it to recognize all the three hydrophobic regions described by Liu and Yao [35] within the PB1 binding site, compound **3** is shifted toward the opposite side of the cavity and matches only the first hydrophobic region, generated by W706. Nevertheless, compound **3** establishes a very favorable H-bond between its C-2 amidic carbonyl group and the Q408 residue, which could be the reason for its efficient inhibition of PA-PB1 heterodimerization.



**Scheme 6.** Synthetic route of the target compound **12** and **21**. Reagents and conditions: (a) thiourea, EtOH, reflux; (b) 2-bromoacetamide, DIPEA, DMF, rt; (c) compound **30** or **31**,  $\text{CH}_2\text{Cl}_2$ , DIPEA, rt.

In the present study, additional hybrid compounds were synthesized as analogues of compound **3** (compounds **5–18**, Fig. 2) and compound **4** (compounds **19–26**, Fig. 2). By mainly focusing on the cHTC core, various structural modifications were undertaken investigating the cycloheptane, the thiophene and the 2-carboxamide moieties. From the antiviral activity, SAR insights were obtained with the main indication entailing the favorable replacement of the cHTC core by a simpler 2-carbamoylphenyl moiety. In depth studies were pursued to determine the ability of the compounds to interfere with RdRP functions, their metabolic stability as well as to predict their binding mode within the  $\text{PA}_C$  cavity. Further studies were also performed on a couple of regioisomers to investigate the different behavior in inhibiting PA-PB1 interaction and viral growth.

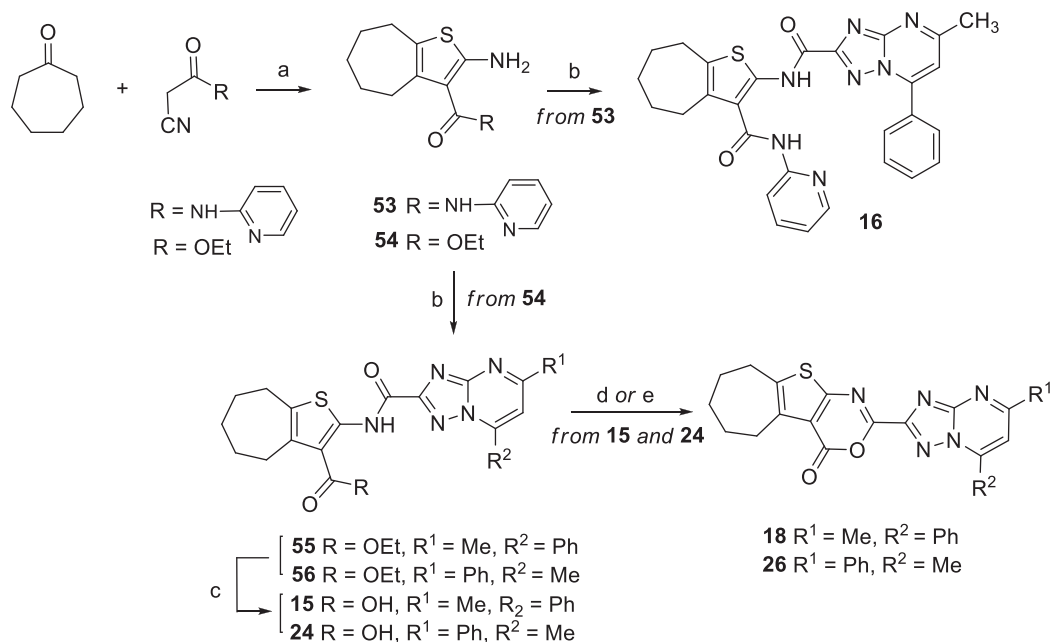
## 2. Results and discussion

### 2.1. Chemistry

The synthesis of all the target compounds **5–13**, **15–22** and **24–29** was accomplished, as reported in Schemes 2–8, by coupling reaction of the appropriate reagent with 5-methyl-7-phenyl-[1,2,4]triazolo[1,5-*a*]pyrimidine-2-carbonyl chloride **30** [32] or 7-methyl-5-phenyl-[1,2,4]triazolo[1,5-*a*]pyrimidine-2-carbonyl chloride **31** [32]. As shown in Scheme 1, derivatives **30** and **31** were obtained by chlorination of the corresponding carboxylic acids [32], which were in turn prepared by cyclocondensation of ethyl 5-amino-1,2,4-triazole-3-carboxylate [36] and 1-phenylbutane-1,3-dione in acetic acid at reflux furnishing ethyl 5-methyl-7-phenyl-[1,2,4]triazolo[1,5-*a*]pyrimidine-2-carboxylate [37] and ethyl 7-methyl-5-phenyl-[1,2,4]triazolo[1,5-*a*]pyrimidine-2-carboxylate [37], followed by basic hydrolysis.

The synthesis of tetrahydrobenzothiophene- (**5** and **19**), cyclopentathiophene- (**6** and **20**), 4,5-dimethylthiophene- (**7**), 6-ethyltetrahydrobenzothieno- (**8**), and benzothiophene- (**9**) 3-carboxamide derivatives entailed the preparation of reagents **36** [38], **37** [38], **38** [39], **39** [40], and **40** [41], respectively (Scheme 2). In particular, compounds **36–39** were obtained by applying the one-pot Gewald reaction entailing the reaction of alkyl ketones **32–35** with cyanoacetamide in the presence of sulphur and *N,N*-diethylamine or morpholine in EtOH. Then, by using conditions different from those reported in literature [41], compound **40** was obtained by oxidation of **39** by using *p*-chloranil in 1,4-dioxane. Coupling reaction of intermediates **36–39** with **30** and intermediates **36** and **37** with **31** in  $\text{CH}_2\text{Cl}_2$  in the presence of *N,N*-diisopropylethylamine (DIPEA) provided the target compounds **5–8**, **19** and **20**.

The synthesis of cHTC derivative **10** entailed the preparation of key intermediate **45**, as reported in Scheme 3. The preparation of



**Scheme 7.** Synthetic route of the target compounds **15**, **24**, **18** and **26**. Reagents and conditions: (a) sulphur, *N,N*-diethylamine, EtOH, rt; (b) compound **30** or **31**, CH<sub>2</sub>Cl<sub>2</sub>, DIPEA, rt; (c) LiOH, H<sub>2</sub>O/THF (1:1), 50 °C; (d) Ac<sub>2</sub>O, 100 °C; (e) DIPEA, EDC, HOBT, CH<sub>2</sub>Cl<sub>2</sub>, from 0 °C to rt.

thiophene-2-carboxamide derivatives was reported in literature by straight reaction of 2-chloro-cyanoderivatives with 2-mercaptoacetamide [42]. However, difficulties in the preparation of the latter as well as its commercial availability led us to undertake a different synthetic route entailing the preparation of ethyl carboxylate intermediate **43** and its successive transformation into carboxamide derivative **45**. In particular, cycloheptanone was reacted with DMF and POCl<sub>3</sub> to give intermediate **41** [43] that was used for the preparation of compound **42** [44] by reaction with hydroxylamine hydrochloride in *N*-methyl-2-pyrrolidinone (NMP). Intermediate **42** was then reacted with ethyl thioglycolate in presence of K<sub>2</sub>CO<sub>3</sub> in a MeOH/THF mixture, to give compound **43** [45]. In order to convert the ethyl carboxylate moiety of compound **43** into a carboxamide group, it was reacted with hydrazine hydrate at 80 °C to give carbonylhydrazide derivative **44**, which was then treated with Ni-Raney in DMF at 90 °C providing compound **45**. Coupling reaction of **45** with **30** furnished the target derivative **10**.

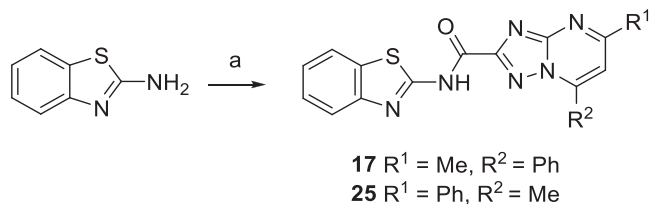
Through an analogous procedure, benzothienopyridine-2-carboxamide derivative **11** and thiophene-2-carboxamide derivatives **13** and **22** were prepared as reported in Schemes 4 and 5, respectively. Thus, ethyl carboxylate derivative **46** [46], prepared by reacting 2-chlorobenzonitrile and ethyl thioglycolate in presence of KOH in DMF, and methyl 3-aminothiophene-2-carboxylate were reacted with hydrazine hydrate providing carbonylhydrazide derivatives **47** [47] and **49** [47], which were in turn treated with Ni-Raney to give carboxamide derivatives **48** [48] and **50** [49],

respectively. Coupling reaction of **48** with **30** and **50** with **30** and **31** provided derivatives **11**, **13** and **22**, respectively.

Thienopyridine-2-carboxamide derivatives **12** and **21** were prepared, as reported in Scheme 6, by coupling reaction of **30** and **31**, respectively, with carboxamide derivative **52** [50], which was obtained by reaction of 2-chloroniconitrile and thiourea in EtOH at reflux to give intermediate **51**, followed by reaction with 2-bromoacetamide in DMF in the presence of DIPEA.

A one-pot Gewald reaction was initially applied for the synthesis of derivatives **16** bearing a C-3 pyridin-2-yl-carbamoyl moiety, **15** and **24** characterized by a C-3 carboxylic acid, and cycloheptathienooxazinones **18** and **26** (Scheme 7). Thus, cycloheptanone was reacted with 2-cyano-*N*-pyridin-2-ylacetamide [51] and ethyl 2-cyanoacetate, providing intermediates **53** [29] and **54** [52], respectively. Reagent **53** was then coupled with **30** to give target compound **16**, while reagent **54** was reacted with **30** and **31** yielding ethyl ester intermediates **55** and **56**, respectively. Hydrolysis under basic conditions of **55** and **56** provided acid derivatives **15** and **24**, which were in turn cyclized to give tricyclic derivatives **18** and **26**. Cyclization of acid **15** was performed in acetic anhydride at 100 °C providing **18** in very low yield (19%). As a consequence, cyclization of **24** was performed through an alternative procedure entailing the use of EDC, DIPEA, and 1-hydroxybenzotriazole in CH<sub>2</sub>Cl<sub>2</sub>, which permitted to obtain derivative **26** in 52% yield.

Finally, benzothiazole derivatives **17** and **25** were synthesized as reported in Scheme 8, by coupling reaction of 2-aminobenzothiazole with **30** and **31**, respectively.

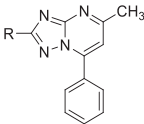
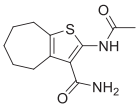
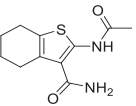
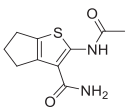
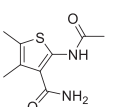
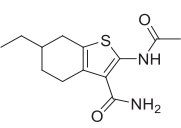
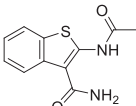
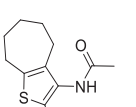
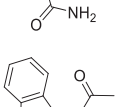
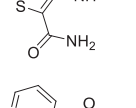
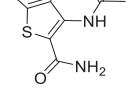


**Scheme 8.** Synthetic route of the target compounds **17** and **25**. Reagents and conditions: (a) compound **30** or **31**, CH<sub>2</sub>Cl<sub>2</sub>, DIPEA, rt.

## 2.2. Inhibition of PA-PB1 heterodimerization and evaluation of anti-Flu activity

The study started from hit compound **3**, considering its better ability to interfere with PA-PB1 interaction. In particular, compounds **5–18** (Table 1) were synthesized by structurally modifying the cycloheptane, the thiophene, and the 2-carboxamide moieties of compound **3**, while keeping the 5-methyl-7-phenyl-[1,2,4]triazolo[1,5-*a*]pyrimidine-2-carboxamide portion.

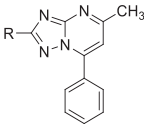
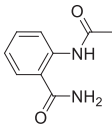
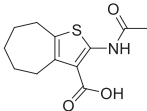
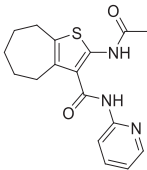
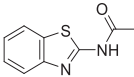
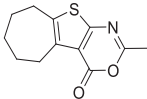
**Table 1**  
Structure and biological activity of compound **3** analogues.

Compd	R			
		ELISA PA-PB1 Interaction Assay IC <sub>50</sub> , μM <sup>a</sup>	PRA in MDCK cells EC <sub>50</sub> , μM <sup>b</sup>	Cytotoxicity in MDCK cells CC <sub>50</sub> , μM <sup>c</sup>
<b>3</b>		1.1 ± 0.3	21 ± 4	>250
<b>5</b>		15 ± 3	32 ± 8	>250
<b>6</b>		6.2 ± 0.3	22 ± 7	>250
<b>7</b>		>200	>50	>250
<b>8</b>		>200	15 ± 2	>250
<b>9</b>		>200	49 ± 1	>250
<b>10</b>		>200	>50	90 ± 7
<b>11</b>		>200	22 ± 4	>250
<b>12</b>		3.3 ± 0.7	>100	>250
<b>13</b>		31 ± 5	43 ± 2	250

(continued on next page)



Table 1 (continued)

Compd	R			
		ELISA PA-PB1 Interaction Assay IC <sub>50</sub> , μM <sup>a</sup>	PRA in MDCK cells EC <sub>50</sub> , μM <sup>b</sup>	Cytotoxicity in MDCK cells CC <sub>50</sub> , μM <sup>c</sup>
14		11 ± 3	>100	>250
15		19 ± 1	50 ± 3	>250
16		23 ± 2	48 ± 2	>250
17		21 ± 1	>50	>250
18		19 ± 1	26 ± 1	101 ± 2
<b>RBV</b>			10 ± 2	>250
<b>Tat-PB1<sub>1-15</sub> peptide</b>		35 ± 4	41 ± 5	>100

<sup>a</sup> Activity of the compounds in ELISA PA-PB1 interaction assays. The IC<sub>50</sub> value represents the compound concentration that reduces by 50% the interaction between PA and PB1.

<sup>b</sup> Activity of the compounds in plaque reduction assays with the Flu A/PR/8/34 strain. The EC<sub>50</sub> value represents the compound concentration that inhibits 50% of plaque formation.

<sup>c</sup> Cytotoxicity of the compounds in MTT assays. The CC<sub>50</sub> value represents the compound concentration that causes a decrease of cell viability of 50%. All the reported values represent the means ± SD of data derived from at least three independent experiments in duplicate.

All the compounds were evaluated for their ability to inhibit the PA-PB1 subunits interaction in an ELISA-based assay, including the Tat-PB1<sub>1-15</sub> peptide as a positive control, and for the antiviral activity in FluA virus-infected MDCK cells by plaque reduction assays (PRA) with the A/PR/8/34 (PR8) strain, using ribavirin (RBV), a known inhibitor of RNA viruses polymerase, as a positive control. To exclude that the observed antiviral activities could be due to toxic effects in the target cells, all the compounds were tested in parallel by MTT assays in MDCK cells.

Regarding the modifications made on the cycloheptane ring, size reduction from cycloheptathiophene to tetrahydrobenzothiophene (compound **5**) and cyclopentathiophene (compound **6**) provided compounds showing a comparable anti-Flu activity (EC<sub>50</sub> = 32 and 22 μM, respectively, vs 21 μM of **3**) but a slightly decreased ability to inhibit PA-PB1 interaction (IC<sub>50</sub> = 15 and 6.2 μM, respectively) with respect to **3** (IC<sub>50</sub> = 1.1 μM). On the other hand, the deletion of the cycloheptane ring gave 4,5-dimethylthiophene **7** devoid of both the activities. The alkylation and aromatization of the tetrahydrobenzene of compound **5** were explored in 6-ethyl-tetrahydrobenzothiophene **8** and

benzothiophene **9**, respectively, which were both endowed with anti-Flu activity (EC<sub>50</sub> = 15 and 49 μM, respectively) but devoid of the ability to disrupt PA-PB1 interaction. Of note, derivative **8** emerged as the most active anti-Flu compound herein reported, even more than hit compound **3**. These results suggested that the presence of a cycloalkyl moiety fused to the thiophene ring is important to obtain anti-Flu activity, although its aromatization is still tolerated but detrimental for anti-PA-PB1 activity.

Then, a set of four derivatives was synthesized in which the thiophene-based core was linked to the TZP moiety by the C-3 position. The thienopyridine derivative **12** was the most potent PA-PB1 inhibitor among the compounds herein reported (IC<sub>50</sub> of 3.3 μM), but at the expense of the antiviral activity (EC<sub>50</sub> > 100 μM), while derivative **13** exhibited a balanced biological profile (IC<sub>50</sub> of 31 μM and EC<sub>50</sub> of 43 μM). These results indicated that, in this series of compounds, the lack of a cycloalkyl ring fused to the thiophene does not impair the activity.

No anti-PA-PB1 activity was shown by cycloheptathiophene compound **10** and benzothiophene compound **11**, the strict analogues of compounds **3** and **9**, respectively, although the latter

**Table 2**  
Structure and biological activity of compound **4** analogues.

Compd	R	ELISA PA-PB1 Interaction Assay IC <sub>50</sub> , μM <sup>d</sup>	PRA in MDCK cells EC <sub>50</sub> , μM <sup>b</sup>	Cytotoxicity in MDCK cells CC <sub>50</sub> , μM <sup>c</sup>
<b>4</b>		28 ± 1	8 ± 2	>250
<b>19</b>		N.D. <sup>d</sup>	N.D.	N.D.
<b>20</b>		N.D.	N.D.	N.D.
<b>21</b>		>200	43 ± 7	51 ± 1
<b>22</b>		50 ± 28	>100	240 ± 8
<b>23</b>		7 ± 1	31 ± 10	>250
<b>24</b>		18 ± 11	70 ± 15	>250
<b>25</b>		>200	40 ± 13	233 ± 5
<b>26</b>		15 ± 5	40 ± 6	>50
<b>RBV</b>			10 ± 2	>250
<b>Tat-PB1<sub>1-15</sub> peptide</b>		35 ± 4	41 ± 5	>100

For the definition of <sup>a</sup> IC<sub>50</sub>, <sup>b</sup> EC<sub>50</sub>, and <sup>c</sup> CC<sub>50</sub>, see Table 1 <sup>d</sup> N.D. = not determined due to solubility issues.

showed anti-Flu activity (EC<sub>50</sub> = 22 μM) comparable to that of hit compound **3** (EC<sub>50</sub> = 21 μM). Of note, the whole cHTC core can be replaced by a simpler benzene ring to achieve anti-PA-PB1 activity, as shown by the 2-carbamoylphenyl derivative **14** [53], characterized by a good IC<sub>50</sub> of 11 μM but devoid of anti-Flu activity. Finally, in order to explore the role of the C-3 carboxamide moiety, it was replaced by a bioisosteric carboxylic group or by an *N*-(2-pyridyl)-carboxamide moiety, which also characterized hit compound **1**, as

in derivatives **15** and **16**, respectively. Moreover, a benzothiazole replaced the cycloheptathiophene ring in derivative **17**, while the two amide linkages at the C-2 and C-3 positions of the cycloheptathiophene were constrained into a 1,3-oxazinone ring in the tricyclic derivative **18**. The four compounds showed a comparable anti-PA-PB1 activity, with IC<sub>50</sub>s ranging from 19 to 23 μM, and compounds **15** and **16** also shared a similar anti-Flu activity (EC<sub>50</sub> = 50 and 48 μM, respectively). The benzothiazole ring



different due to the presence of selective weak interactions that stabilize the two crystal structures. Particularly, the distortion of the structure of **23** is caused by the presence of a relatively strong intermolecular hydrogen bond between H1Nb and N3 (2.275 Å), while the phenyl substituent on **14** is involved in multiple intermolecular  $\pi$  interactions with the phenyl moieties of other molecules of **14** causing a parallel displaced  $\pi$  -  $\pi$  stacking (planes distance 3.710 Å, centroids distance 4.072 Å) [59], which provides a stabilization of the three-dimensional crystal lattice. In the latter case thus, the molecular packing can be attributed also to the formation of favorable interactions between neighboring aromatic side chains. The established interactions and consequently the different molecular packing may account for a substantial amount of the crystal stabilization. Accordingly, as they account for many characteristics of compounds, such as solubility, these features may justify the differences into the solubility values for compounds **14** and **23**, which could have compromised the antiviral evaluation.

#### 2.4. In depth characterization of compound **23**

##### 2.4.1. Inhibition of flu RdRP activity in a minireplicon assay

Then we investigated whether the compound ability to disrupt the PA-PB1 interaction *in vitro* correlated with the ability to interfere with the catalytic activity of FluA RdRP in a cellular context, by disrupting the correct assembly of the polymerase complex. To this aim, a minireplicon assay was performed for compound **23**. 293T cells were co-transfected with plasmids for the expression of FluA nucleoprotein (NP), PA, PB1, and PB2 proteins and the firefly luciferase RNA, flanked by the noncoding regions of Flu A/WSN/33 segment 8, in the presence of the test compound or DMSO as a control. The expression of the firefly reporter gene indicates that a negative-sense RNA is synthesized and is reconstituted intracellularly into functional vRNP in which all four NP, PA, PB1, and PB2 proteins are co-expressed and interact with each other. Compound **23** exhibited a potent inhibitory effect on FluA polymerase activity, showing an  $EC_{50}$  of  $5.8 \pm 2.0$   $\mu$ M, and thus being more effective than RBV ( $24 \pm 4$   $\mu$ M). These data confirmed the ability of compound **23** to inhibit RdRP functions by interfering with PA-PB1 heterodimerization.

##### 2.4.2. Metabolic stability in human liver microsomes

Metabolic stability in human liver microsomes (HLM) was studied by monitoring the percentage of unchanged substrate and the formation of the metabolite(s) at five time points (0, 10, 20, 40 and 60 min). LC-MS raw data were analyzed by using MassMetasite (version 3.3.6; Molecular Discovery Ltd., Middlesex, UK) [60,61] and WebMetabase (version 4.0.6; Molecular Discovery Ltd., Middlesex, UK) [62,63] software for automatic metabolite identification and structure elucidation as well as for kinetic analysis. After 60 min incubation, the 76% of compound **23** was in its unchanged form, indicating a good metabolic stability. In addition, the kinetic analysis performed in WebMetabase allowed to estimate the half-life value and the intrinsic clearance for compound **23**, as 166 min and  $4.18$   $\mu$ L/min\*  $mg_{prot}$ , respectively (Fig. S1, supporting information). The analysis of formed metabolites allowed for the detection of one metabolite only, obtained by an aromatic hydroxylation reaction at the 2-carboxybenzamide moiety (Fig. S2, supporting information). Although the MS/MS fragmentation is not sufficient to identify the exact position of the site of metabolism in the aromatic ring, the most probable site for hydroxylation appears to be at C-4 position, according to MetaSite [64] predictions within the WebMetabase analysis tool (Table S3 and Fig. S3, supporting information).

##### 2.4.3. Human plasma protein binding

Regarding the human plasma protein binding, samples were analyzed by employing a rapid equilibrium system device and adding them in buffer and measuring the compound presence in the human plasma compartment after 4 h of incubation by means of UPLC/MS/MS. It was observed that compound **23** showed an unbound fraction of 22.45%, which together with the good metabolic stability predicts a good bioavailability of the compound in human plasma.

##### 2.4.4. Computational studies

Finally, with the aim to gain information on how two different moieties, such as the cHTC and the 2-carbamoylphenyl, showed a favorable ability to disrupt PA-PB1 interaction, computational studies were performed to predict the binding mode of benzamide derivative **23** within the PA cavity with respect to hit compound **4**. For comparative purpose, also its isomer **14**, which was active in ELISA-based assay but devoid of any antiviral activity, was studied in comparison to hit compound **3**.

The study was conducted using the same method applied for the evaluation of the binding mode of compounds **3** and **4** using the FLAP software [65], and the most probable binding poses for the two isomers are illustrated in Fig. 4. In agreement with the biological results, both compounds showed an efficient binding within the PA<sub>C</sub>, although through different orientations and interactions. In particular, both compounds were found to efficiently interact with W706 through hydrophobic interactions, as observed for all the inhibitors of the PA-PB1 interaction we have studied so far [24].

Similarly to **4**, compound **23** displayed a favorable hydrophobic interaction with all the three hydrophobic regions previously described by Liu and Yao [35]. Indeed, according to the proposed description of the protein cavity, the first hydrophobic region is centered on residues W706 and F411, the second one is defined by F710 and L666, and the third one includes L640, V636, M595, and W619. However, differently from **4**, **23** seems to be involved in the formation of a favorable H-bond between the 2-carboxamide NH group and the hydroxyl group of T639. This amino acid was not found to be involved in such kind of interaction in other compounds studied so far by us.

Concerning compound **14**, the hydrophobic interaction occurs only in the first hydrophobic pocket, in a similar fashion to **3**. Differently from **3**, a favored H-bonding with Q408 was established with the 2-carboxamide carbonyl group instead of the carbonyl group of the amide linking the TZP and the phenyl ring. However, according to the GRID fields analysis in FLAP, for **14** the replacement of the cycloheptathiophene moiety with the phenyl ring led to a slightly different orientation that facilitates the formation of a second H-bond with I621, one of the key residues of PA in binding of PB1 (data not shown). Nevertheless, this slight change in the pose results in a reduced  $\pi$ - $\pi$  interaction. This data seems to confirm the importance of an efficient interaction with W706 for inhibition of PA-PB1 heterodimerization.

In conclusion, the computational study confirmed the central interaction between the inhibitors and W706, and the 2-carboxamide group of **23** and **14** was pivotal in the interaction with PA by establishing favorable H-bonds. This is also experimentally confirmed, since the analogues lacking the 2-carboxamide substituent showed a very weak activity in the ELISA PA-PB1 interaction assays [32].

### 3. Conclusions

The Flu RdRP is emerging as a privileged drug-target as demonstrated by the most recently approved compounds or in the pipeline such as favipiravir, baloxavir marboxil and pimidivir,

which act by inhibiting each of the three RdRP subunits.

By applying an alternative approach to inhibit Flu RdRP functions, since many years we have been working on the development of compounds able to interfere with RdRP subunits interaction and in particular with PA-PB1 heterodimerization. cHTC and TZP emerged among the best scaffolds able to disrupt this interaction, and their merging led us to identify interesting hybrid compounds (**3** and **4**). Starting from these hits, in this work, two sets of analogues were synthesized by maintaining the TZP core while deeply modifying the cHTC moiety. Some promising compounds showed the ability to interfere with the PA-PB1 interaction, such as cyclopentathiophene derivative **6** ( $IC_{50} = 6.2 \mu M$ ), phenyl derivative **23** ( $IC_{50} = 7 \mu M$ ) and cycloheptathienooxazinones **18** and **26** ( $IC_{50} = 19$  and  $15 \mu M$ , respectively), coupled with good anti-Flu activity ( $EC_{50}$  ranging from 22 to  $40 \mu M$ ). On the other hand, some compounds showed only anti-Flu activity ( $EC_{50} = 15\text{--}50 \mu M$ ) leading to hypothesize a different mechanism of action, or only anti-PA-PB1 activity ( $IC_{50} = 3.3\text{--}50 \mu M$ ). To investigate this latter behavior, chemical/physical properties were determined for the couple of isomers **14** and **23** both showing anti-PA-PB1 activity but only **23** having anti-Flu properties. Compound **14** showed a lower equilibrium solubility with respect to **23**, which could arise from a major molecular packing, as shown by X-Ray studies, which may account for a substantial amount of the crystal stabilization. In particular, the phenyl ring at the C-7 position of the TZP nucleus is involved in multiple intermolecular  $\pi\text{-}\pi$  interactions with the phenyl moieties of other molecules causing stabilization of the three-dimensional crystal lattice. These data confirmed one of the main drawbacks of PPI inhibitors that, interacting with interfaces generally flat and highly hydrophobic, often suffer from low solubility. In agreement, the  $PA_C$  cavity is characterized by hydrophobic regions and hydrophobic interactions are indispensable to achieve an efficient small molecule-PA binding. Computational studies performed on compounds **14** and **23** confirmed the crucial hydrophobic interaction between the TZP core and W706 for inhibition of PA-PB1 heterodimerization. Nevertheless, favorable H-bonds seem to contribute to the interaction of the compounds with the  $PA_C$ .

This work furnished important structure insights that could be exploited for the design of further analogues, also endowed with better drug-like properties. Indeed, the good biological and chemical/physical properties shown by compound **23**, in which a simpler phenyl ring replaced the cycloheptathiophene, highlighted the possibility to reduce unnecessary hydrophobic moieties. A further increase of the hydrophilicity of the compounds could be also achieved by a structure-based drug design aimed at introducing polar groups establishing favorable H-bonds with the  $PA_C$ .

## 4. Experimental section

### 4.1. Chemistry

Commercially available starting materials, reagents, and solvents were used as supplied. All reactions were routinely monitored by TLC on silica gel 60F254 (Merck) and visualized by using UV or iodine. Flash column chromatography was performed on Merck silica gel 60 (mesh 230–400). After extraction, organic solutions were dried over anhydrous  $Na_2SO_4$ , filtered, and concentrated with a Büchi rotary evaporator at reduced pressure. Yields are of purified product and were not optimized. HRMS spectra were registered on Agilent Technologies 6540 UHD Accurate Mass Q-TOF LC/MS, HPLC 1290 Infinity. Purities of target compounds were determined by HPLC Waters LC Module I Plus and evaluated to be higher than 95% (at both 254 (reported below in the description of the compounds) and 296 nm). In order to evaluate their stability, the purity was also determined by HPLC analysis monitored at

296 nm after eleven days, and it was over 95%. HPLC conditions to assess the purity of final compounds were as follows: column: XTerra MS C18 column reversed-phase ( $3.5 \mu$  spherical hybrid,  $4.6 \text{ mm} \times 150 \text{ mm}$ ,  $3.5 \mu m$  particle size); flow rate, 0.8 mL/min; acquisition time, 10 min; isocratic elution, mobile phase: acetonitrile 80%, water 20%, formic acid 0.1%.  $^1H$  NMR and  $^{13}C$  NMR spectra were recorded on Bruker Avance DRX-400MHz using residual solvents such as dimethylsulfoxide ( $\delta = 2.48$ ) or chloroform ( $\delta = 7.26$ ) as an internal standard. Chemical shifts were recorded in ppm ( $\delta$ ) and the spectral data are consistent with the assigned structures. The spin multiplicities are indicated by the: symbols s (singlet), d (doublet), t (triplet), m (multiplet), and bs (broad singlet).

#### 4.1.1. 2-Amino-6-ethyl-4,5,6,7-tetrahydrobenzo[b]thiophene-3-carboxamide (**39**)

[40] A mixture of 4-ethylcyclohexanone (0.5 g, 3.96 mmol) 2-cyanoacetamide (0.35 g, 4.16 mmol) and sulphur (0.13 g, 4.16 mmol) in ethanol (5 mL) was heated to reflux. Morpholine (0.36 g, 4.16 mmol) was added dropwise to the heating solution and the mixture was allowed to heat to reflux 4 h. After cooling, the reaction mixture was poured into ice/water obtaining a precipitate which was filtered and treated with cyclohexane, to give **39** (0.7 g, 79%);  $^1H$  NMR (DMSO- $d_6$ , 400 MHz):  $\delta$  0.86 (t,  $J = 7.4$  Hz, 3H,  $CH_2CH_3$ ), 1.16–1.35 (m, 4H,  $CH_2CH_3$  and cyclohexane  $CH_2$ ), 1.45–1.55, 1.77–1.80 and 2.00–2.06 (m, each 1H, cyclohexane CH), 2.51–2.57 (m, 2H, cyclohexane  $CH_2$ ), 6.48 (bs, 2H,  $CONH_2$ ), 6.86 (s, 2H,  $NH_2$ ).

#### 4.1.2. 2-Aminobenzo[b]thiophene-3-carboxamide (**40**)

[41] A mixture of **36** [38] (0.5 g, 2.55 mmol) and *p*-chloroanil (1.25 g, 5.10 mmol) in 1,4-dioxane (30 mL) was heated at  $90^\circ C$  for 4 h. After cooling, the reaction mixture was filtered over Celite and the filtrate was evaporated to dryness, to give a residue that was stirred with saturated  $NaHCO_3$  solution for 15 min. The solution was then extracted with  $CH_2Cl_2$  and the organic layers were evaporated to dryness to give a grey solid, which was purified by flash chromatography eluting with MeOH/ $CH_2Cl_2$  (2%), to give **9** (0.29 g, 59%);  $^1H$  NMR (DMSO- $d_6$ , 200 MHz):  $\delta$  6.80–6.95 (m, 3H, benzothiophene CH and  $NH_2$ ), 7.15–7.20 (t,  $J = 7.15$  Hz, 1H, benzothiophene CH), 7.50–7.60 (m, 4H, aromatic CH and  $CONH_2$ ).

#### 4.1.3. General procedure for carbodiimide formation (method A)

To a solution of 5-methyl-7-phenyl-[1,2,4]triazolo[1,5-*a*]pyrimidine-2-carboxylic acid [37] or 5-methyl-7-phenyl-[1,2,4]triazolo[1,5-*a*]pyrimidine-2-carboxylic acid [37] (1.0 equiv) in well dry  $CH_2Cl_2$ , oxalyl chloride (3 equiv) was added and after 30 min dry DMF (2 drops) was added. After 2 h, the reaction mixture was evaporated to dryness to give **30** [37] or **31** [37] that was dissolved in well dry  $CH_2Cl_2$  and added of the appropriate amine (1.0 equiv) and DIPEA (1.0 equiv). The reaction mixture was maintained at r. t. until no starting material was detected by TLC. Then, it was worked up through two procedures: (procedure 1) the reaction mixture was evaporated to dryness to give a residue that was poured into ice/water providing a precipitate which was filtered and purified as reported in the description of the compounds; or (procedure 2) the precipitate formed in the reaction mixture was filtered and purified as reported in the description of the compounds.

#### 4.1.4. *N*-(3-carbamoyl-4,5,6,7-tetrahydrobenzo[b]thiophen-2-yl)-5-methyl-7-phenyl-[1,2,4]triazolo[1,5-*a*]pyrimidine-2-carboxamide (**5**)

The title compound was prepared starting from **36** [38] and **30** [37] through method A (4 h), worked up through procedure 1, and purified by flash chromatography eluting with MeOH/ $CHCl_3$  (2%), in 57% yield as orange solid.  $^1H$  NMR (DMSO- $d_6$ , 400 MHz):  $\delta$  1.60–1.70

(m, 4H, cyclohexane CH<sub>2</sub>), 2.40–2.75 (m, 7H, cyclohexane CH<sub>2</sub> and CH<sub>3</sub>), 7.60–7.70 (m, 4H, phenyl CH and H-6), 8.10–8.20 (m, 2H, phenyl CH), 13.00 (s, 1H, NHCO); <sup>13</sup>C NMR (DMSO-*d*<sub>6</sub>, 101 MHz): δ 22.7, 22.8, 24.3, 25.3, 25.6, 112.3, 117.8, 127.6, 129.1, 129.7, 129.8, 130.0, 132.1, 141.7, 147.1, 155.7, 156.0, 157.6, 167.3, 167.6; HRMS: *m/z* calcd for C<sub>22</sub>H<sub>20</sub>N<sub>6</sub>O<sub>2</sub>S 433.1402 (M + H)<sup>+</sup>, found 433.144661 (M + H)<sup>+</sup>. HPLC, ret. time: 2.755 min, peak area: 98.70%.

#### 4.1.5. *N*-(3-carbamoyl-5,6-dihydro-4*H*-cyclopenta[*b*]thiophen-2-yl)-5-methyl-7-phenyl-[1,2,4]triazolo[1,5-*a*]pyrimidine-2-carboxamide (6)

The title compound was prepared starting from **37** [38] and **30** [37] through method A (4 h), worked up through procedure 1, and purified by flash chromatography eluting with MeOH/CHCl<sub>3</sub> (2%), in 63% yield as yellow solid. <sup>1</sup>H NMR (DMSO-*d*<sub>6</sub>, 400 MHz): δ 2.30–2.40 (m, 2H, cyclopentane CH<sub>2</sub>), 2.70 (s, 3H, CH<sub>3</sub>), 2.75–2.85 and 2.90–3.00 (m, each 2H, cyclopentane CH<sub>2</sub>), 6.60 (bs, 1H, CONH<sub>2</sub>), 7.55–7.70 (m, 5H, phenyl CH, H-6 and CONH<sub>2</sub>), 8.10–8.20 (m, 2H, phenyl CH), 13.25 (s, 1H, NHCO); <sup>13</sup>C NMR (DMSO-*d*<sub>6</sub>, 101 MHz): δ 25.3, 28.1, 28.7, 29.4, 112.3, 112.9, 129.1, 129.7, 130.0, 132.2, 133.3, 139.9, 147.1, 147.3, 155.7, 156.0, 157.4, 167.3; HRMS: *m/z* calcd for C<sub>21</sub>H<sub>18</sub>N<sub>6</sub>O<sub>2</sub>S 419.1291 (M + H)<sup>+</sup>, found 419.128947 (M + H)<sup>+</sup>. HPLC, ret. time: 2.655 min, peak area: 99.12%.

#### 4.1.6. *N*-(3-carbamoyl-4,5-dimethylthiophen-2-yl)-5-methyl-7-phenyl-[1,2,4]triazolo[1,5-*a*]pyrimidine-2-carboxamide (7)

The title compound was prepared starting from **38** [66] and **30** [37] through method A (3 h), worked up through procedure 1, and purified by flash chromatography eluting with MeOH/CHCl<sub>3</sub> (2%) and then washed with hot DMF, in 30% yield as yellow solid. <sup>1</sup>H NMR (DMSO-*d*<sub>6</sub>, 200 MHz): δ 2.15 and 2.20 (s, each 3H, thiophene CH<sub>3</sub>), 2.60 (s, 3H, CH<sub>3</sub>), 7.60–7.70 (m, 4H, phenyl CH and H-6), 8.10–8.20 (m, 2H, phenyl CH), 12.75 (s, 1H, NHCO); <sup>13</sup>C NMR (DMSO-*d*<sub>6</sub>, 101 MHz): δ 12.6, 13.8, 25.2, 112.3, 119.7, 124.5, 127.8, 129.1, 129.6, 129.9, 132.1, 139.9, 147.0, 155.6, 155.9, 157.4, 167.3, 167.7; HRMS: *m/z* calcd for C<sub>20</sub>H<sub>18</sub>N<sub>6</sub>O<sub>2</sub>S 407.1291 (M + H)<sup>+</sup>, found 407.12883 (M + H)<sup>+</sup>. HPLC, ret. time: 2.522 min, peak area: 95.37%.

#### 4.1.7. *N*-(3-carbamoyl-6-ethyl-4,5,6,7-tetrahydrobenzo[*b*]thiophen-2-yl)-5-methyl-7-phenyl-[1,2,4]triazolo[1,5-*a*]pyrimidine-2-carboxamide (8)

The title compound was prepared starting from **39** [40] and **30** [37] through method A (3 h), worked up through procedure 1, and purified by flash chromatography eluting with MeOH/CHCl<sub>3</sub> (2%) and then treated with EtOH, in 60% yield as yellow solid. <sup>1</sup>H NMR (DMSO-*d*<sub>6</sub>, 400 MHz): δ 0.90 (t, *J* = 7.3 Hz, 3H, CH<sub>2</sub>CH<sub>3</sub>), 1.30–1.40 (m, 3H, cyclohexane CH<sub>2</sub>), 1.50–1.60, 1.80–1.90, and 2.20–2.30 (m, each 1H, cyclohexane CH<sub>2</sub>), 2.65–2.75 (m, 6H, CH<sub>2</sub>CH<sub>3</sub>, cyclohexane CH, and CH<sub>3</sub>), 7.50–7.60 (m, 6H, phenyl CH, H-6, and CONH<sub>2</sub>), 8.10–8.20 (m, 2H, phenyl CH), 13.00 (s, 1H, NHCO); <sup>13</sup>C NMR (DMSO-*d*<sub>6</sub>, 101 MHz): δ 11.7, 25.2, 25.3, 28.4, 28.6, 30.2, 35.7, 112.2, 117.4, 127.3, 129.1, 129.6, 129.6, 129.9, 132.1, 141.8, 147.0, 155.6, 155.9, 157.4, 167.3, 167.5; HRMS: *m/z* calcd for C<sub>24</sub>H<sub>24</sub>N<sub>6</sub>O<sub>2</sub>S 461.1760 (M + H)<sup>+</sup>, found 461.175597 (M + H)<sup>+</sup>. HPLC, ret. time: 3.322 min, peak area: 96.12%.

#### 4.1.8. *N*-(3-carbamoylbenzo[*b*]thiophen-2-yl)-5-methyl-7-phenyl-[1,2,4]triazolo[1,5-*a*]pyrimidine-2-carboxamide (9)

The title compound was prepared starting from **40** [41] and **30** [37] through method A (1 h), worked up through procedure 2, and purified by flash chromatography eluting with MeOH/CHCl<sub>3</sub> (2%), in 47% yield as yellow solid; <sup>1</sup>H NMR (DMSO-*d*<sub>6</sub>, 400 MHz): δ 2.75 (s, 3H, CH<sub>3</sub>), 7.30 and 7.45 (t, *J* = 7.5 Hz, each 1H, benzothiophene CH), 7.60–7.70 (m, 4H, phenyl CH and H-6), 7.85 (bs, 2H, CONH<sub>2</sub>), 7.95–8.05 and 8.10–8.20 (m, each 2H, phenyl CH and

benzothiophene CH), 13.50 (s, 1H, NHCO); <sup>13</sup>C NMR (DMSO-*d*<sub>6</sub>, 101 MHz): δ 25.2, 112.2, 112.4, 122.5, 122.9, 124.2, 125.7, 129.1, 129.5, 130.0, 132.2, 133.3, 134.0, 145.7, 147.1, 155.9, 156.8, 157.1, 167.3, 167.5; HRMS: *m/z* calcd for C<sub>22</sub>H<sub>16</sub>N<sub>6</sub>O<sub>2</sub>S 429.1134 (M + H)<sup>+</sup>, found 429.113549 (M + H)<sup>+</sup>. HPLC, ret. time: 2.633 min, peak area: 95.48%.

#### 4.1.9. *N*-(3-carbamoyl-4,5,6,7-tetrahydrobenzo[*b*]thiophen-2-yl)-7-methyl-5-phenyl-[1,2,4]triazolo[1,5-*a*]pyrimidine-2-carboxamide (19)

The title compound was prepared starting from **36** [38] and **31** [37] through method A (overnight), worked up through procedure 2, and purified by flash chromatography eluting with MeOH/CHCl<sub>3</sub> (2%), in 30% yield as light yellow solid; <sup>1</sup>H NMR (DMSO-*d*<sub>6</sub>, 400 MHz): δ 1.73–1.75 (m, 4H, cyclohexane CH<sub>2</sub>), 2.60–2.65 and 2.70–2.75 (m, each 2H, cyclohexane CH<sub>2</sub>), 2.85 (s, 3H, CH<sub>3</sub>), 7.55–7.60 (m, 3H, phenyl CH), 8.10 (s, 1H, H-6), 8.25–8.30 (m, 2H, phenyl CH), 13.10 (s, 1H, NHCO); <sup>13</sup>C NMR (DMSO-*d*<sub>6</sub>, 101 MHz): δ 17.3, 22.7, 22.8, 24.2, 25.5, 109.2, 117.7, 127.6, 128.1, 129.5, 129.7, 132.0, 136.1, 141.6, 149.6, 155.2, 155.6, 157.9, 161.7, 167.5; HRMS: *m/z* calcd for C<sub>22</sub>H<sub>20</sub>N<sub>6</sub>O<sub>2</sub>S 433.1447 (M + H)<sup>+</sup>, found 433.144794 (M + H)<sup>+</sup>. HPLC, ret. time: 2.806 min, peak area: 99.79%.

#### 4.1.10. *N*-(3-carbamoyl-5,6-dihydro-4*H*-cyclopenta[*b*]thiophen-2-yl)-7-methyl-5-phenyl-[1,2,4]triazolo[1,5-*a*]pyrimidine-2-carboxamide (20)

The title compound was prepared starting from **37** [38] and **31** [37] through method A (overnight), worked up through procedure 2, and purified by flash chromatography eluting with MeOH/CHCl<sub>3</sub> (2%), in 45% yield as yellow solid; <sup>1</sup>H NMR (DMSO-*d*<sub>6</sub>, 400 MHz): δ 2.30 (quin, *J* = 7.2 Hz, 2H, cyclopentane CH<sub>2</sub>), 2.80 (t, *J* = 7.2 Hz, 2H, cyclopentane CH<sub>2</sub>), 2.85 (s, 3H, CH<sub>3</sub>), 2.95 (t, *J* = 7.2 Hz, 2H, cyclopentane CH<sub>2</sub>), 7.55–7.60 (m, 3H, phenyl CH), 8.05 (s, 1H, H-6), 8.25–8.30 (m, 2H, phenyl CH), 13.40 (s, 1H, NHCO); <sup>13</sup>C NMR (DMSO-*d*<sub>6</sub>, 101 MHz): δ 17.3, 28.1, 28.7, 29.5, 109.2, 117.7, 127.0, 128.1, 128.9, 129.5, 131.8, 133.4, 139.9, 149.5, 155.6, 156.4, 158.1, 162.0, 167.2; HRMS: *m/z* calcd for C<sub>21</sub>H<sub>18</sub>N<sub>6</sub>O<sub>2</sub>S 419.1291 (M + H)<sup>+</sup>, found 419.128962 (M + H)<sup>+</sup>. HPLC, ret. time: 3.069 min, peak area: 95.51%.

#### 4.1.11. General procedure for hydrazide formation (method B)

A mixture of the appropriate reagent (0.5 g) and hydrazine hydrate (10 mL) was heated at 80 °C for 3 h. After cooling, the precipitate obtained was filtered and washed with water.

#### 4.1.12. 3-Amino-5,6,7,8-tetrahydro-4*H*-cyclohepta[*b*]thiophene-2-carbohydrazide (44)

The title compound was prepared starting from **43** [45] through Method B in 99% yield; <sup>1</sup>H NMR (CDCl<sub>3</sub>, 400 MHz): δ 1.50–1.70 (m, 6H, cycloheptane CH<sub>2</sub>), 2.40–2.45 (m, 2H, cycloheptane CH<sub>2</sub>), 2.70–2.75 (m, 2H, cycloheptane CH<sub>2</sub>), 3.70 (bs, 2H, NHNH<sub>2</sub>), 5.60 (s, 2H, NH<sub>2</sub>), 6.50 (s, 1H, NHNH<sub>2</sub>).

#### 4.1.13. General procedure for hydrazide reduction (method C)

A mixture of the appropriate hydrazine and a catalytic amount of Ni-Raney in DMF was heated at 90 °C for until no starting material was detected by TLC. After cooling, the reaction mixture was filtered over Celite and the filtrate was evaporated to dryness to give a residue, which was purified as reported below in the description of the compounds.

#### 4.1.14. 3-Amino-5,6,7,8-tetrahydro-4*H*-cyclohepta[*b*]thiophene-2-carboxamide (45)

The title compound was prepared starting from **44** through Method C (3 h), after purification by treatment with Et<sub>2</sub>O, in 54% yield; <sup>1</sup>H NMR (DMSO-*d*<sub>6</sub>, 200 MHz): δ 1.25–1.50 (m, 6H, cycloheptane CH<sub>2</sub>), 1.60–1.75 (m, 2H, cycloheptane CH<sub>2</sub>), 2.50–2.60 (m,

2H, cycloheptane CH<sub>2</sub>), 6.30 (s, 2H, NH<sub>2</sub>), 6.60 (s, 2H, CONH<sub>2</sub>).

**4.1.15. N-(2-carbamoyl-5,6,7,8-tetrahydro-4H-cyclohepta[b]thiophen-3-yl)-5-methyl-7-phenyl-[1,2,4]triazolo[1,5-a]pyrimidine-2-carboxamide (10)**

The title compound was prepared starting from **45** and **30** [37] through Method A (overnight), worked up through procedure 1, and purified by flash chromatography eluting with acetone/CHCl<sub>3</sub> (30%), in 48% yield as yellow solid; <sup>1</sup>H NMR (DMSO-*d*<sub>6</sub>, 400 MHz): δ 1.40–1.50, 1.55–1.65, 1.75–1.85 and 2.35–2.45 (m, each 2H, cycloheptane CH<sub>2</sub>), 2.65 (s, 3H, CH<sub>3</sub>), 2.70–2.80 (m, 2H, cycloheptane CH<sub>2</sub>), 7.30 (bs, 2H, CONH<sub>2</sub>), 7.50–7.70 (m, 4H, aromatic CH and H-6), 8.15–8.20 (m, 2H, aromatic CH) 10.75 (s, 1H, NHCO); <sup>13</sup>C NMR (DMSO-*d*<sub>6</sub>, 101 MHz): δ 25.3, 27.2, 28.0, 28.3, 30.7, 32.2, 79.5, 112.2, 124.1, 129.1, 129.7, 130.0, 132.1, 135.9, 136.8, 139.5, 142.7, 147.1, 155.9, 158.4, 158.6, 163.6, 167.2; HRMS: *m/z* calcd for C<sub>23</sub>H<sub>22</sub>N<sub>6</sub>O<sub>2</sub>S 447.1604 (M + H)<sup>+</sup>, found 447.16086 (M + H)<sup>+</sup>. HPLC, ret. time: 2.559 min, peak area: 96.88%.

**4.1.16. 3-Aminobenzo[b]thiophene-2-carboxamide (48)**

[48] The title compound was prepared starting from **46** [46] through Method B providing **47** [47] in 72% yield, followed by Method C (4 h, purification by treatment with Et<sub>2</sub>O) in 46% yield; <sup>1</sup>H NMR (DMSO-*d*<sub>6</sub>, 200 MHz): δ 6.95–7.00 (m, 4H, CONH<sub>2</sub> and NH<sub>2</sub>), 7.25–7.40 (m, 2H, aromatic CH), 7.70 (d, *J* = 7.66 Hz, 1H, aromatic CH), 7.90 (d, *J* = 8.25 Hz, 1H, aromatic CH).

**4.1.17. N-(2-carbamoylbenzo[b]thiophen-3-yl)-5-methyl-7-phenyl-[1,2,4]triazolo[1,5-a]pyrimidine-2-carboxamide (11)**

The title compound was prepared starting from **48** [48] and **30** [37] through Method A (4 h), worked up through procedure 1, and purified by flash chromatography eluting with MeOH/CHCl<sub>3</sub> (2%), in 40% yield as yellow solid; <sup>1</sup>H NMR (DMSO-*d*<sub>6</sub>, 400 MHz): δ 2.75 (s, 3H, CH<sub>3</sub>), 7.40 (t, *J* = 7.6 Hz, 1H, aromatic CH), 7.45 (t, *J* = 7.1 Hz, 1H, aromatic CH), 7.60–7.70 (m, 3H, aromatic CH), 7.70 (s, 1H, H-6), 7.75 (d, *J* = 8.1 Hz, 1H, aromatic CH), 7.80 (bs, 2H, CONH<sub>2</sub>), 8.00 (d, *J* = 8.1 Hz, 1H, aromatic CH), 8.15–8.20 (m, 2H, aromatic CH), 11.70 (bs, 1H, NHCO); <sup>13</sup>C NMR (DMSO-*d*<sub>6</sub>, 101 MHz): δ 25.3, 79.6, 112.3, 123.4, 125.0, 127.3, 128.2, 129.2, 129.7, 130.0, 131.7, 132.2, 135.2, 137.1, 147.1, 156.0, 158.4, 164.0, 167.2; HRMS: *m/z* calcd for C<sub>22</sub>H<sub>16</sub>N<sub>6</sub>O<sub>2</sub>S 429.1134 (M + H)<sup>+</sup>, found 429.112694 (M + H)<sup>+</sup>. HPLC, ret. time: 2.384 min, peak area: 99.97%.

**4.1.18. 3-Aminothiophene-2-carboxamide (50)**

[49] The title compound was prepared starting from methyl 3-aminothiophene-2-carboxylate through Method B providing **49** [47] in 100% yield, followed by Method C (overnight, purification by treatment with Et<sub>2</sub>O) in 20% yield; <sup>1</sup>H NMR (DMSO-*d*<sub>6</sub>, 400 MHz): δ 6.38 (s, 2H, NH<sub>2</sub>), 6.52 (d, *J* = 4.8 Hz, 1H, thiophene CH), 6.81 (s, 2H, NH<sub>2</sub>), 7.32 (d, *J* = 4.8 Hz, 1H, thiophene CH).

**4.1.19. N-(2-carbamoylthiophen-3-yl)-5-methyl-7-phenyl-[1,2,4]triazolo[1,5-a]pyrimidine-2-carboxamide (13)**

The title compound was prepared starting from **50** [49] and **30** [37] through Method A (1 h), worked up through procedure 1, and purified by flash chromatography eluting with MeOH/CHCl<sub>3</sub> (2%), in 38% yield as yellow solid; <sup>1</sup>H NMR (DMSO-*d*<sub>6</sub>, 400 MHz): δ 2.70 (s, 1H, CH<sub>3</sub>), 7.65–7.65 (m, 4H, aromatic CH and H-6), 7.80 and 8.10 (d, *J* = 5.4 Hz, each 1H, thiophene CH), 8.15–8.20 (m, 2H, aromatic CH), 12.70 (s, 1H, NHCO); <sup>13</sup>C NMR (DMSO-*d*<sub>6</sub>, 101 MHz): δ 25.2, 112.1, 114.9, 122.0, 127.2, 129.1, 129.6, 130.0, 132.1, 141.8, 147.0, 156.0, 156.4, 158.2, 165.6, 167.1; HRMS: *m/z* calcd for C<sub>18</sub>H<sub>14</sub>N<sub>6</sub>O<sub>2</sub>S 379.0977 (M + H)<sup>+</sup>, found 379.097525 (M + H)<sup>+</sup>. HPLC, ret. time: 2.317 min, peak area: 99.85%.

**4.1.20. N-(2-carbamoylthiophen-3-yl)-7-methyl-5-phenyl-[1,2,4]triazolo[1,5-a]pyrimidine-2-carboxamide (22)**

The title compound was prepared starting from **50** [49] and **31** [37] through Method A (overnight), worked up through procedure 1, and purified by flash chromatography eluting with MeOH/CHCl<sub>3</sub> (4%), in 36% yield as yellow solid; <sup>1</sup>H NMR (DMSO-*d*<sub>6</sub>, 400 MHz): δ 2.80 (s, 1H, CH<sub>3</sub>), 7.50–7.60 (m, 4H, aromatic CH and CONH<sub>2</sub>), 7.80 (d, *J* = 5.3 Hz, 1H, thiophene CH), 8.10 (s, 1H, H-6), 8.15 (d, *J* = 5.3 Hz, 1H, thiophene CH), 8.25–8.30 (m, 3H, aromatic CH and CONH<sub>2</sub>), 12.90 (s, 1H, NHCO); <sup>13</sup>C NMR (DMSO-*d*<sub>6</sub>, 101 MHz): δ 17.3, 109.1, 114.9, 122.1, 127.9, 128.1, 129.5, 132.0, 136.2, 141.8, 149.5, 155.3, 156.4, 158.7, 161.7, 165.6; HRMS: *m/z* calcd for C<sub>18</sub>H<sub>14</sub>N<sub>6</sub>O<sub>2</sub>S 379.0977 (M + H)<sup>+</sup>, found 379.09724. HPLC, ret. time: 4.093 min, peak area: 95.93%.

**4.1.21. 3-(5-Methyl-7-phenyl-[1,2,4]triazolo[1,5-a]pyrimidine-2-carboxamido)thieno[2,3-b]pyridine-2-carboxamide (12)**

The title compound was prepared starting from **52** [50] and **30** [37] through Method A (overnight), worked up through procedure 1, and purified by flash chromatography eluting with MeOH/CHCl<sub>3</sub> (3%), in 60% yield as yellow solid; <sup>1</sup>H NMR (DMSO-*d*<sub>6</sub>, 400 MHz): δ 2.70 (s, 3H, CH<sub>3</sub>), 7.50 (dd, *J* = 4.6 and 8.3 Hz, 1H, aromatic CH), 7.60–7.65 (m, 3H, aromatic CH), 7.70 (s, 1H, H-6), 7.95 (bs, 2H, CONH<sub>2</sub>), 8.15–8.20 (m, 2H, aromatic CH), 8.30 (dd, *J* = 1.6 and 8.3 Hz, 1H, aromatic CH), 8.65 (dd, *J* = 1.6 Hz and 4.4 Hz, 1H, aromatic CH), 11.70 (s, 1H, NHCO); <sup>13</sup>C NMR (DMSO-*d*<sub>6</sub>, 101 MHz): δ 25.3, 112.3, 120.5, 124.9, 128.7, 129.2, 129.7, 130.0, 131.0, 132.2, 134.2, 147.1, 149.9, 156.1, 157.8, 158.1, 158.2, 164.1, 167.3; HRMS: *m/z* calcd for C<sub>21</sub>H<sub>15</sub>N<sub>7</sub>O<sub>2</sub>S 430.1087 (M + H)<sup>+</sup>, found 430.108031 (M + H)<sup>+</sup>. HPLC, ret. time: 2.284 min, peak area: 97.41%.

**4.1.22. 3-(7-Methyl-5-phenyl-[1,2,4]triazolo[1,5-a]pyrimidine-2-carboxamido)thieno[2,3-b]pyridine-2-carboxamide (21)**

The title compound was prepared starting from **52** [50] and **31** [37] through Method A (1 h), worked up through procedure 2, and purified by flash chromatography eluting with MeOH/CHCl<sub>3</sub> (5%), in 54% yield as yellow solid; <sup>1</sup>H NMR (DMSO-*d*<sub>6</sub>, 400 MHz): δ 2.85 (s, 3H, CH<sub>3</sub>), 7.50–7.55 (m, 1H, aromatic CH), 7.60–7.65 (m, 3H, aromatic CH), 7.70 (bs, 2H, CONH<sub>2</sub>), 8.15 (s, 1H, H-6), 8.30–8.35 (m, 3H, aromatic CH), 8.70–8.75 (m, 1H, aromatic CH), 11.70 (s, 1H, NHCO); <sup>13</sup>C NMR (DMSO-*d*<sub>6</sub>, 101 MHz): δ 17.3, 109.2, 120.5, 125.4, 128.1, 128.7, 129.5, 130.7, 132.0, 134.1, 136.1, 149.6, 149.8, 155.3, 157.7, 158.1, 158.6, 161.7, 163.9; HRMS: *m/z* calcd for C<sub>21</sub>H<sub>15</sub>N<sub>7</sub>O<sub>2</sub>S 430.1087 (M + H)<sup>+</sup>, found 430.108391 (M + H)<sup>+</sup>. HPLC, ret. time: 2.319 min, peak area: 96.26%.

**4.1.23. 5-Methyl-7-phenyl-N-(3-(pyridin-2-ylcarbamoyl)-5,6,7,8-tetrahydro-4H-cyclohepta[b]thiophen-2-yl)-[1,2,4]triazolo[1,5-a]pyrimidine-2-carboxamide (16)**

The title compound was prepared starting from **53** [29] and **30** [37] through Method A (overnight), worked up through procedure 1, and purified by treatment with Et<sub>2</sub>O, in 97% yield as yellow solid. <sup>1</sup>H NMR (DMSO-*d*<sub>6</sub>, 400 MHz): δ 1.50–1.70 (m, 4H, cycloheptane CH<sub>2</sub>), 1.75–1.85 (m, 2H, cycloheptane CH<sub>2</sub>), 2.65 (s, 3H, CH<sub>3</sub>), 2.70–2.75 and 2.80–2.85 (m, each 2H, cycloheptane CH<sub>2</sub>), 7.15–7.20 (m, 1H, aromatic CH), 7.55–7.70 (m, 4H, aromatic CH and H-6), 7.80–7.85 (m, 1H, aromatic CH), 8.10–8.15 (m, 2H, aromatic CH), 8.20–8.25 and 8.30–8.35 (m, each 1H, aromatic CH), 10.25 and 11.50 (s, each 1H, NHCO); <sup>13</sup>C NMR (DMSO-*d*<sub>6</sub>, 101 MHz): δ 25.2, 27.3, 27.8, 28.7, 31.9, 112.3, 115.0, 120.4, 123.0, 129.0, 129.6, 129.9, 132.1, 132.2, 135.9, 136.8, 138.5, 147.1, 148.5, 151.9, 155.8, 155.9, 157.3, 164.7, 167.4; HRMS: *m/z* calcd for C<sub>28</sub>H<sub>25</sub>N<sub>7</sub>O<sub>2</sub>S 524.1869 (M + H)<sup>+</sup>, found 524.186282 (M + H)<sup>+</sup>. HPLC, ret. time: 4.344 min, peak area: 98.46%.

4.1.24. Ethyl 2-(5-methyl-7-phenyl-[1,2,4]triazolo[1,5-a]pyrimidine-2-carboxamido)-5,6,7,8-tetrahydro-4H-cyclohepta[b]thiophene-3-carboxylate (55)

The title compound was prepared starting from **54** [52] and **30** [37] through Method A (1 h), worked up through procedure 1, and purified by flash chromatography eluting with acetone/CHCl<sub>3</sub> (5%), in 61% yield; <sup>1</sup>H NMR (DMSO-*d*<sub>6</sub>, 400 MHz): δ 1.30 (t, *J* = 7.1 Hz, 3H, CH<sub>2</sub>CH<sub>3</sub>), 1.50–1.65 (m, 4H, cycloheptane CH<sub>2</sub>), 1.70–1.80 (m, 2H, cycloheptane CH<sub>2</sub>), 2.65–2.75 (m, 5H, cycloheptane CH<sub>2</sub> and CH<sub>3</sub>), 3.00–3.10 (m, 2H, cycloheptane CH<sub>2</sub>), 4.30 (q, *J* = 7.1 Hz, 2H, CH<sub>2</sub>CH<sub>3</sub>), 7.55–7.70 (m, 4H, aromatic CH and H-6), 8.10–8.20 (m, 2H, aromatic CH), 12.40 (s, 1H, NHCO).

4.1.25. Ethyl 2-(7-methyl-5-phenyl-[1,2,4]triazolo[1,5-a]pyrimidine-2-carboxamido)-5,6,7,8-tetrahydro-4H-cyclohepta[b]thiophene-3-carboxylate (56)

The title compound was prepared starting from **54** [52] and **31** [37] through Method A (1 h), worked up through procedure 2, and purified by treatment by EtOAc/EtOH mixture, in 56% yield; <sup>1</sup>H NMR (DMSO-*d*<sub>6</sub>, 400 MHz): δ 1.30 (t, *J* = 7.1 Hz, 3H, CH<sub>2</sub>CH<sub>3</sub>), 1.50–1.65 (m, 4H, cycloheptane CH<sub>2</sub>), 1.70–1.80 (m, 2H, cycloheptane CH<sub>2</sub>), 2.65–2.70 (m, 2H, cycloheptane CH<sub>2</sub>), 2.80 (s, 3H, CH<sub>3</sub>), 2.90–3.00 (m, 2H, cycloheptane CH<sub>2</sub>), 4.30 (q, *J* = 7.1 Hz, 2H, CH<sub>2</sub>CH<sub>3</sub>), 7.55–7.60 (m, 3H, aromatic CH), 8.05 (s, 1H, H-6), 8.20–8.25 (m, 2H, aromatic CH), 12.40 (s, 1H, NHCO).

4.1.26. 2-(5-Methyl-7-phenyl-[1,2,4]triazolo[1,5-a]pyrimidine-2-carboxamido)-5,6,7,8-tetrahydro-4H-cyclohepta[b]thiophene-3-carboxylic acid (15)

A suspension of **55** (0.33 g, 0.69 mmol) and LiOH (0.11 g, 2.77 mmol) in a mixture H<sub>2</sub>O/THF (1:1) was maintained at 50 °C for 24 h. After cooling the reaction mixture was acidified (pH 4–5) with 2 N HCl obtaining a precipitate that was filtered and purified by flash chromatography eluting with MeOH/CHCl<sub>3</sub> (3%) to give **15** (0.25 g, 80% yield) as yellow solid; <sup>1</sup>H NMR (DMSO-*d*<sub>6</sub>, 400 MHz): δ 1.35–1.60 (m, 4H, cycloheptane CH<sub>2</sub>), 1.70–1.80 (m, 2H, cycloheptane CH<sub>2</sub>), 2.60–2.70 (m, 5H, cycloheptane CH<sub>2</sub> and CH<sub>3</sub>), 3.20–3.30 (m, 2H, cycloheptane CH<sub>2</sub>), 7.60–7.70 (m, 4H, aromatic CH and H-6), 8.10–8.20 (m, 2H, aromatic CH), 14.50 (bs, 1H, COOH); <sup>13</sup>C NMR (DMSO-*d*<sub>6</sub>, 101 MHz): δ 25.2, 27.3, 27.7, 28.3, 28.8, 32.8, 112.0, 121.0, 129.1, 129.7, 130.0, 130.1, 132.1, 139.0, 140.4, 147.0, 155.5, 155.9, 158.4, 167.0; HRMS: *m/z* calcd for C<sub>23</sub>H<sub>21</sub>N<sub>5</sub>O<sub>2</sub>S 448.14441 (M + H)<sup>+</sup>, found 448.143999 (M + H)<sup>+</sup>. HPLC, ret. time: 3.303 min, peak area: 98.83%.

4.1.27. 2-(7-Methyl-5-phenyl-[1,2,4]triazolo[1,5-a]pyrimidine-2-carboxamido)-5,6,7,8-tetrahydro-4H-cyclohepta[b]thiophene-3-carboxylic acid (24)

The title compound was prepared starting from **56** through the procedure used for the synthesis of **15** in 58% yield; <sup>1</sup>H NMR (DMSO-*d*<sub>6</sub>, 400 MHz): δ 1.50–1.55 (m, 4H, cycloheptane CH<sub>2</sub>), 1.75–1.80 and 2.65–2.70 (m, each 2H, cycloheptane CH<sub>2</sub>), 2.85 (s, 3H, CH<sub>3</sub>), 3.05–3.10 (m, 2H, cycloheptane CH<sub>2</sub>), 7.60–7.70 (m, 3H, aromatic CH), 8.10 (s, 1H, H-6), 8.20–8.25 (m, 2H, aromatic CH). <sup>13</sup>C NMR (DMSO-*d*<sub>6</sub>, 101 MHz): δ 17.3, 27.2, 27.5, 27.9, 28.5, 32.3, 109.1, 122.1, 128.0, 129.5, 131.2, 132.0, 135.6, 136.1, 138.0, 149.5, 155.2, 155.6, 158.0, 161.8, 167.5. HRMS: *m/z* calcd for C<sub>23</sub>H<sub>21</sub>N<sub>5</sub>O<sub>3</sub>S 448.14441 (M + H)<sup>+</sup>, found 448.14375 (M + H)<sup>+</sup>. HPLC, ret. time: 5.832 min, peak area: 100%.

4.1.28. 2-(5-Methyl-7-phenyl-[1,2,4]triazolo[1,5-a]pyrimidin-2-yl)-6,7,8,9-tetrahydro-4H,5H-cyclohepta[4,5]thieno[2,3-*d*] [1,3]oxazin-4-one (18)

A mixture of **15** (0.33 g, 0.73 mmol) and acetic anhydride (0.78 g, 7.7 mmol) was heated at 100 °C for 30 h. After cooling, the reaction

mixture was poured into ice/water obtaining a precipitate that was filtered and crystallized by EtOH/DMF, to give **18** (0.06 g, 19%); <sup>1</sup>H NMR (DMSO-*d*<sub>6</sub>) δ: 1.60–1.65 (m, 4H, cycloheptane CH<sub>2</sub>), 1.80–1.85 (m, 2H, cycloheptane CH<sub>2</sub>), 2.70 (s, 3H, CH<sub>3</sub>), 2.85–2.90 and 3.10–3.15 (m, each 2H, cycloheptane CH<sub>2</sub>), 7.60–7.65 (m, 4H, H-6 and aromatic CH), 8.10–8.15 (m, 2H, aromatic CH); <sup>13</sup>C NMR (101 MHz, DMSO-*d*<sub>6</sub>) δ: 25.2, 26.9, 27.5, 27.7, 29.5, 32.0, 112.4, 118.8, 129.1, 129.7, 129.8, 132.0, 137.9, 141.2, 146.9, 151.6, 154.7, 156.2, 156.6, 158.3, 167.2; HRMS: *m/z* calcd for C<sub>23</sub>H<sub>19</sub>N<sub>5</sub>O<sub>2</sub>S 430.1338 (M + H)<sup>+</sup>, found 430.133443 (M + H)<sup>+</sup>. HPLC, ret. time: 3.875 min, peak area: 98.83%.

4.1.29. 2-(7-Methyl-5-phenyl-[1,2,4]triazolo[1,5-a]pyrimidin-2-yl)-6,7,8,9-tetrahydro-4H,5H-cyclohepta[4,5]thieno[2,3-*d*] [1,3]oxazin-4-one (26)

To a suspension of **24** (0.04 g, 0.089 mmol) in dry CH<sub>2</sub>Cl<sub>2</sub>, a solution of EDC hydrochloride (0.017 g, 0.089 mmol), DMAP (0.011 g, 0.089 mmol), and HOBt monohydrate (0.013 g, 0.089 mmol) in CH<sub>2</sub>Cl<sub>2</sub> was added dropwise at 0 °C. The reaction mixture was maintained at rt for 24 h and, then, it was evaporated to dryness providing a residue that was purified by flash chromatography eluting with MeOH/CHCl<sub>3</sub> (2%), to give **26** (0.02 g, 52%); <sup>1</sup>H NMR (DMSO-*d*<sub>6</sub>) δ: 1.65–1.60 (m, 4H, cycloheptane CH<sub>2</sub>), 1.80–1.85 (m, 2H, cycloheptane CH<sub>2</sub>), 2.80–2.90 (m, 5H, cycloheptane CH<sub>2</sub> and CH<sub>3</sub>), 3.10–3.15 (m, 2H, cycloheptane CH<sub>2</sub>), 7.55–7.60 (m, 3H, aromatic CH), 8.10 (s, 1H, H-6), 8.25–8.30 (m, 2H, aromatic CH); <sup>13</sup>C NMR (101 MHz, DMSO-*d*<sub>6</sub>) δ: 17.4, 26.9, 27.5, 27.7, 29.5, 32.0, 109.1, 118.8, 128.0, 129.6, 132.0, 136.1, 138.0, 141.3, 149.2, 151.6, 154.8, 156.9, 158.4, 161.5, 166.4; HRMS: *m/z* calcd for C<sub>23</sub>H<sub>19</sub>N<sub>5</sub>O<sub>2</sub>S 430.1338 (M + H)<sup>+</sup>, found 430.133652 (M + H)<sup>+</sup>. HPLC, ret. time: 3.652, peak area: 97.58%.

4.1.30. *N*-(benzo[d]thiazol-2-yl)-5-methyl-7-phenyl-[1,2,4]triazolo[1,5-a]pyrimidine-2-carboxamide (17)

The title compound was prepared starting from 2-aminobenzothiazole and **30** [37] through Method A (72 h), worked up through procedure 1, and purified by flash chromatography eluting with acetone/CHCl<sub>3</sub> (5%), in 36% yield as yellow solid; <sup>1</sup>H NMR (DMSO-*d*<sub>6</sub>, 400 MHz): δ 2.70 (s, 3H, CH<sub>3</sub>), 7.30 (t, *J* = 7.4 Hz, 1H, aromatic CH), 7.40 (t, *J* = 7.3 Hz, 1H, aromatic CH), 7.55–7.70 (m, 4H, aromatic CH and H-6), 7.80 (d, *J* = 7.9 Hz, 1H, aromatic CH), 8.10 (d, *J* = 7.7 Hz, 1H, aromatic CH), 8.20–8.30 (m, 2H, aromatic CH), 13.10 (bs, 1H, NHCO); <sup>13</sup>C NMR (DMSO-*d*<sub>6</sub>, 101 MHz): δ 25.3, 112.4, 121.0, 122.3, 124.5, 126.8, 129.2, 129.5, 130.1, 131.9, 132.2, 147.1, 156.1, 156.4, 157.6, 158.1, 159.4, 167.4; HRMS: *m/z* calcd for C<sub>20</sub>H<sub>11</sub>N<sub>6</sub>O<sub>2</sub>S 387.1029 (M + H)<sup>+</sup>, found 387.102196 (2 M + H)<sup>+</sup>. HPLC, ret. time: 3.278 min, peak area: 98.8%.

4.1.31. *N*-(Benzo[d]thiazol-2-yl)-7-methyl-5-phenyl-[1,2,4]triazolo[1,5-a]pyrimidine-2-carboxamide (25)

The title compound was prepared starting from 2-aminobenzothiazole and **31** [37] through Method A (72 h), worked up through procedure 2, and purified by crystallization by DMF, in 57% yield as yellow solid; <sup>1</sup>H NMR (DMSO-*d*<sub>6</sub>, 400 MHz): δ 2.85 (s, 1H, CH<sub>3</sub>), 7.35 and 7.45 (t, *J* = 7.6 Hz, each 1H, aromatic CH), 7.55–7.60 (m, 3H, aromatic CH), 7.80 and 8.00 (d, *J* = 8.0 Hz, each 1H, aromatic CH), 8.10 (s, 1H, H-6), 8.25–8.30 (m, 2H, aromatic CH), 13.0 (s, 1H, NHCO); <sup>13</sup>C NMR (DMSO-*d*<sub>6</sub>, 101 MHz): δ 17.3, 109.3, 121.0, 122.2, 124.4, 126.7, 128.1, 129.5, 131.9, 132.0, 136.1, 148.3, 149.5, 155.3, 158.0, 151.1, 159.4, 161.8; HRMS: *m/z* calcd for C<sub>20</sub>H<sub>11</sub>N<sub>6</sub>O<sub>2</sub>S 387.1029 (M + H)<sup>+</sup>, found 387.1022 (M + H)<sup>+</sup>. HPLC, ret. time: 2.898 min, peak area: 99.85%.



## 4.2. Computational methods

The binding poses of compounds **23** and **14** in the PA cavity were generated using the FLAP software (version 2.2.1, Molecular Discovery Ltd., Middlesex, UK; [www.moldiscovery.com](http://www.moldiscovery.com)); the procedure has been extensively described elsewhere [26,27,29]. The main cavity of the crystallographic structure of a large C-terminal fragment of PA (aa 257–716) (pdb code: 3CM8) [21] was used as a template. A total of 50 conformers for each ligand was generated to mimic the compound flexibility, and the most abundant protonation state of each molecule was used, as predicted by MoKa [67]. The probes used to generate the GRID Molecular Interaction Fields were H (shape), DRY (hydrophobic interactions), N1 (H-bond donor) and O (H-bond acceptor) interactions.

## 4.3. Biology

### 4.3.1. Compounds and peptide

RBV (1-D-ribofuranosyl-1,2,4-triazole-3-carboxamide) was purchased from Roche. Each test compound was dissolved in 100% DMSO. The PB1<sub>(1–15)</sub>–Tat peptide was synthesized and purified by the Peptide Facility of CRIBI Biotechnology Center (University of Padua, Padua, Italy). This peptide corresponds to the first 15 amino acids of PB1 protein fused to a short sequence of HIV Tat protein (amino acids 47–59), which allows the delivery into the cell [68].

### 4.3.2. Cells and virus

Mardin-Darby canine kidney (MDCK) and human embryonic kidney (HEK) 293T cells were grown in Dulbecco's modified Eagle's medium (DMEM, Life Technologies) supplemented with 10% (v/v) fetal bovine serum (FBS, Life Technologies) and antibiotics (100 U/mL penicillin and 100 µg/mL streptomycin, Life Technologies). Cells were maintained at 37 °C in a humidified atmosphere with 5% CO<sub>2</sub>. Influenza virus strain A/PR/8/34 (H1N1, Cambridge lineage) was kindly provided by P. Digard (Roslin Institute, University of Edinburgh, United Kingdom).

### 4.3.3. PA–PB1 interaction enzyme-linked immunosorbent assay (ELISA)

The PA–PB1 interaction was detected by a procedure previously described [27]. Briefly, 96-well microtiter plates (Nuova Aptca) were coated with 400 ng of 6His-PA<sub>(239–716)</sub> for 3 h at 37 °C and then blocked with 2% BSA (Sigma) in PBS for 1 h at 37 °C. The 6His-PA<sub>(239–716)</sub> protein was expressed in *E. coli* strain BL21 (DE3)pLysS and purified as already described [27]. After washing, 200 ng of GST-PB1<sub>(1–25)</sub>, or of GST alone as a control, in the absence or the presence of test compounds at various concentrations, were added and incubated O/N at room temperature. *Escherichia coli*-expressed, purified GST and GST-PB1<sub>(1–25)</sub> proteins were obtained as previously described [27,69]. After washing, the interaction between 6His-PA<sub>(239–716)</sub> and GST-PB1<sub>(1–25)</sub> was detected with a horseradish peroxidase-coupled anti-GST monoclonal antibody (GenScript) diluted 1:4000 in PBS supplemented with 2% FBS. Following washes, the substrate 3,3',5,5'-tetramethylbenzidine (TMB, KPL) was added and absorbance was measured at 450 nm by an ELISA plate reader (Tecan Sunrise™). Values obtained from the samples treated with only DMSO were used to set as 100% of PA–PB1 interaction.

### 4.3.4. Cytotoxicity assay

Cytotoxicity of compounds was tested in MDCK cells by the 3-(4,5-dimethylthiazol-2-yl)-2,5-diphenyl tetrazolium bromide (MTT) method, as previously reported [27,70]. Briefly, MDCK cells (seeded at density of  $2 \times 10^4$  per well) were grown in 96-well plates for 24 h and then treated with serial dilutions of test compounds, or DMSO as a control, in DMEM supplemented with 10% FBS. After

incubation at 37 °C for 48 h, 5 mg/mL of MTT (Sigma) in PBS was added into each well and incubated at 37 °C for further 4 h. Successively, a solubilization solution was added to lyse the cells and incubated O/N at 37 °C. Finally, optical density was read at the wavelength of 620 nm on a microtiter plate reader (Tecan Sunrise™).

### 4.3.5. Plaque reduction assay (PRA)

The antiviral activity of test compounds against influenza A virus was tested by PRA as previously described [27]. MDCK cells were seeded at  $5 \times 10^5$  cells/well into 12-well plates, and incubated at 37 °C for 24 h. The following day, the culture medium was removed and the monolayers were first washed with serum-free DMEM and then infected with the Flu A/PR/8/34 strain at 40 PFU/well in DMEM supplemented with 1 µg/mL of TPCK-treated trypsin (Worthington Biochemical Corporation) and 0.14% BSA and incubated for 1 h at 37 °C. The influenza virus infection was performed in the presence of different concentrations of test compounds or solvent (DMSO) as a control. After virus adsorption, DMEM containing 1 µg/mL of TPCK-treated trypsin, 0.14% BSA, 1.2% Avicel, and DMSO or test compounds was added to the cells. At 48 h post-infection, cells were fixed with 4% formaldehyde and stained with 0.1% toluidine blue. Viral plaques were counted, and the mean plaque number in the DMSO-treated control was set at 100%.

### 4.3.6. Minireplicon assays

The minireplicon assay was performed as described [27], with some modifications. Briefly, HEK 293T cells ( $2 \times 10^5$  cells per well) were plated into 24-well plates and incubated overnight at 37 °C. The next day, cells were transfected using calcium phosphate coprecipitation method with pcDNA-PB1, pcDNA-PB2, pcDNA-PA, pcDNA-NP plasmids (100 ng/well of each) along with 50 ng/well of the pPoll-Flu-ffLuc reporter plasmid and 50 ng/well of pRL-SV40 plasmid as a transfection control. Transfections were performed in the presence of different concentrations of test compounds or DMSO. RBV was used as a positive control for inhibition. Cell medium was removed 5 h post-transfection and replaced with DMEM containing the compounds, RBV, or DMSO. At 24 h post-transfection, cells were harvested, lysed and both firefly and *Renilla* luciferase activity were measured using the Dual Luciferase Assay Kit (Promega). In each experiment, firefly luciferase activity was normalized with that of the *Renilla* luciferase and relative luciferase units (RLU) were obtained. The activity measured in control transfection reactions containing DMSO was set at 100% of polymerase activity.

## 4.4. Equilibrium solubility assay

The stock solutions (10–2 M) of the assayed compounds were diluted to decreased molarity, from 300 µM to 0.1 µM, in 384 well transparent plate (Greiner 781,801) with 1% DMSO: 99% PBS buffer. Then, they were incubate at 37 °C and read after 2 h in a NEPH-ELostar Plus (BMG LABTECH). The results were adjusted to a segmented regression to obtain the maximum concentration in which compounds are soluble. Digossin, prazosin and progesterone were used as reference compounds (equilibrium solubility = 84.0, 62.8 and 6.5 µM, respectively) [71].

## 4.5. X-ray studies

X-Ray diffraction patterns of the crystals were recorded using a Bruker D8 Venture diffractometer equipped with an Incoatec ImuS 3.0 microfocuss sealed-tube Mo K $\alpha$  ( $\lambda = 0.71073$  Å) source and a CCD Photon II detector. The analyses were carried out at 120 (2) K using an Oxford Cryosystems 800 cooler. The data collected through

generic  $\phi$  and  $\omega$  were integrated and reduced using the Bruker AXS V8 Saint Software. The structures were solved and all the thermal parameters were anisotropically refined using the SHELXT and SHELXL packages of the Bruker APEX3 software.

#### 4.6. Human plasma protein binding

The assay was carried out by employing Rapid Equilibrium Dialysis (RED) from Thermo Scientific. The compounds were dissolved at 5  $\mu$ M in plasma (from Seralab) and added to the corresponding insert of the RED device. Dialysis buffer was added to the corresponding insert of the RED device. Plate was incubated for 4 h at 37 °C and, then, 50  $\mu$ L aliquots of each chamber were transferred to empty vials. 50  $\mu$ L of dialysis buffer were added to the plasma samples and 50  $\mu$ L of plasma were added to the buffer samples. 300  $\mu$ L of acetonitrile were added to all the samples and centrifuged at 4000 rpm. Supernatant was taken and analyzed by UPLC/MS/MS for sample quantification. Stationary phase: Reverse phase Acquity UPLC® BEH C18 1.7  $\mu$ m (2.1 mm  $\times$  50 mm) (Waters); mobile phase: 0.1% Formic acid water/0.1% formic acid in acetonitrile; gradient:

Time	Water	Acetonitrile
0	95%	5%
0.1	95%	5%
1	0%	100%
2	0%	100%
2.1	95%	5%
2.5	95%	5%

Flow: 0.6 ml/min. The chromatographic equipment employed was an UPLC QSM Waters Acquity. Compound concentrations were calculated from the MS peak areas.

#### 4.7. Metabolic stability in human liver microsomes

Test compounds (10  $\mu$ M) were preincubated for 5 min at 37 °C in a 0.1 M phosphate buffer (pH 7.4) containing Human Liver Microsomes (1 mg/mL) in a total volume of 500  $\mu$ L. The reactions were initiated by addition of NADPH (2 mM) in a shaking water bath at 37 °C. An aliquot of reactions mixture (75  $\mu$ L) was taken at 0, 10, 20, 40 and 60 min and was added to 75  $\mu$ L of cold acetonitrile (containing 10  $\mu$ M labetalol as an internal standard) to terminate the reaction. Proteins were precipitated by centrifugation at 12 000 g for 5 min at 4 °C (Eppendorf, Italy; centrifuge 5810 R; rotor F-45-30-11), and aliquots of the supernatants were analyzed by LC-MS/MS.

The instrumentation used in this study consisted in an Agilent 6540 UHD Accurate-Mass Quadrupole Time-of-Flight (QTOF), equipped with an Agilent 1290 Infinity LC system (Agilent Technologies, Santa Clara, CA, USA).

The columns was a Phenomenex Luna Omega Polar C18 column (1.6  $\mu$ m, 2.1  $\times$  150 mm). Column temperature was set at 40 °C and injection volume was 5  $\mu$ L. The mobile phases consisted of 0.1% formic acid in water (A) and acetonitrile + 0.1% formic acid (B) and the LC gradient was as follows: 0–10 min 0–95% B, 10–12 min 95–95% B, at a flow rate of 0.4 ml/min. The Agilent Technology 6540 UHD Accurate Mass Q-TOF LC/MS system was operated under positive conditions with Dual JetStream source (ESI source) in the following conditions: Gas Temp 350 °C, Drying Gas: 9 l/min, Nebulizer: 35 psi, Sheath Gas Temp: 400 °C, Sheath Gas Flow: 9 l/min, Vcap: 4000 V, Nozzle Voltage: 0 V, Fragmentor: 120 V, Skimmer: 65 V, OCT RF Vpp: 750 V. The acquisition was performed

in AutoMS/MS mode using a mass list to trigger the MS/MS acquisition based on the accurate masses of potential metabolites as computed by MetaSite software [64]. The AutoMS/MS settings were: MS range: 119–1400  $m/z$ , rate 3 spectra/s; MS/MS range: 100–1400  $m/z$ , Rate 6 spectra/s; Isolation Width: “medium (4  $m/z$ ); Fixed Collision energy 15 V, max 1 precursor Per Cycle, Abs. Precursor threshold 100 counts, Rel Threshold 0.01%. Data Analysis was performed by processing raw data files using Mass-MetaSite (version 3.3.6, Molecular Discovery Ltd., Middlesex, UK, Molecular Discovery Ltd., UK; [www.moldiscovery.com](http://www.moldiscovery.com)) and WebMetabase (version 4.0.6 Molecular Discovery Ltd., Middlesex, UK, Molecular Discovery Ltd., UK; [www.moldiscovery.com](http://www.moldiscovery.com)).

#### Declaration of competing interest

The authors declare that they have no known competing financial interests or personal relationships that could have appeared to influence the work reported in this paper.

#### Acknowledgments

This work was supported by grants “Excellent Departments” by Ministero dell’Istruzione, dell’Università e della Ricerca-MIUR (to S. Massari and A. Donnadio), PRIN 2017 - cod. 2017BMK8JR (to S. Massari, S. Sabatini, and V. Cecchetti), Fondazione Cassa Risparmio Perugia - Ricerca Scientifica e Tecnologica 2019: “Giovani ricercatori: risorsa per il territorio” (to M.C. Pismataro), Associazione Italiana per la Ricerca sul Cancro, AIRC – Fellowships for Italy 2018 (to T. Felicetti), Xunta de Galicia (ED431C 2018/21 & ED431G 2019/02), European Regional Development Fund (ERDF) (to J. Brea), Associazione Italiana per la Ricerca sul Cancro, AIRC, grant n. IG18855 (to A. Loregian); British Society for Antimicrobial Chemotherapy, UK, BSAC-2018-0064 (to A. Loregian), Ministero dell’Istruzione, dell’Università e della Ricerca, PRIN 2017 - cod. 2017KM79NN (to A. Loregian), Fondazione Cassa di Risparmio di Padova e Rovigo - Bando Ricerca Covid-2019 Nr. 55777 2020.0162 (to A. Loregian), and financial support to the project AMIS, through the program “Dipartimento di Eccellenza 2018–2022, by Ministero dell’Istruzione, dell’Università e della Ricerca-MIUR-project AMIS (to L. Goracci and L. Tensi).

#### Appendix A. Supplementary data

Supplementary data to this article can be found online at <https://doi.org/10.1016/j.ejmech.2020.112944>.

Supporting Information. Appendix A. Supplementary data

#### References

- [1] world health organization WHO, Influenza. <http://www.who.int/influenza>. (Accessed 4 September 2020).
- [2] J.K. Taubenberger, J.C. Kash, D.M. Morens, The 1918 influenza pandemic: 100 years of questions answered and unanswered, *Sci. Transl. Med.* 11 (2019) 5485–5501, <https://doi.org/10.1126/scitranslmed.aau5485>.
- [3] Centers for Disease Control and Prevention, Influenza (Flu), Centers for disease control and prevention. <https://www.cdc.gov/flu/avianflu/monitoring-bird-flu.html>, 2017. (Accessed 4 September 2020).
- [4] Z. Beau Reneer, T.M. Ross, H2 influenza viruses: designing vaccines against future H2 pandemics, *Biochem. Soc. Trans.* 47 (2019) 251–264, <https://doi.org/10.1042/BST20180602>.
- [5] R.J. Garten, C.T. Davis, C.A. Russell, B. Shu, S. Lindstrom, A. Balish, W.M. Sessions, X. Xu, E. Skepner, V. Deyde, M. Okomo-Adhiambo, L. Gubareva, J. Barnes, C.B. Smith, S.L. Emery, M.J. Hillman, P. Rivaitter, J. Smagala, M. De Graaf, D.F. Burke, R.A.M. Fouchier, C. Pappas, C.M. Alpuche-Aranda, H. López-Gatell, H. Olivera, I. López, C.A. Myers, D. Faix, P.J. Blair, C. Yu, K.M. Keene, P.D. Dotson, D. Boxrud, A.R. Sambol, S.H. Abid, K. St George, T. Bannerman, A.L. Moore, D.J. Stringer, P. Blevins, G.J. Demmler-Harrison, M. Ginsberg, P. Kriner, S. Waterman, S. Smole, H.F. Guevara, E.A. Belongia, P.A. Clark, S.T. Beatrice, R. Donis, J. Katz, L. Finelli, C.B. Bridges, M. Shaw, D.B. Jernigan, T.M. Uyeki, D.J. Smith, A.I. Klimov, N.J. Cox, Antigenic and genetic

- characteristics of swine-origin 2009 A(H1N1) influenza viruses circulating in humans, *Science* 325 (80–) (2009) 197–201, <https://doi.org/10.1126/science.1176225>.
- [6] W.R. Dowdle, Influenza A virus recycling revisited, *Bull. World Health Organ.* 77 (1999) 820–828.
- [7] Y. Lu, S. Landreth, A. Gaba, M. Hlasny, G. Liu, Y. Huang, Y. Zhou, In vivo characterization of avian influenza A (H5N1) and (H7N9) viruses isolated from canadian travelers, *Viruses* 11 (2019) 193–205, <https://doi.org/10.3390/v11020193>.
- [8] M.G. Ison, Antiviral treatments, *Clin. Chest Med.* 38 (2017) 139–153, <https://doi.org/10.1016/j.ccm.2016.11.008>.
- [9] V. Peltola, E.A. Govorkova, E.A. Hernandez-Vargas, S. Esposito, N. Principi, B. Camilloni, A. Alunno, I. Polinori, A. Argentiero, Drugs for influenza treatment: is there significant news? *Front. Med.* 1 (2019) 109–115, <https://doi.org/10.3389/fmed.2019.00109>.
- [10] M. Toots, R.K. Plemper, Next-generation direct-acting influenza therapeutics, *Transl. Res.* 220 (2020) 33–42, <https://doi.org/10.1016/j.trsl.2020.01.005>.
- [11] F.G. Hayden, N. Shindo, Influenza virus polymerase inhibitors in clinical development, *Curr. Opin. Infect. Dis.* 32 (2019) 176–186, <https://doi.org/10.1097/QCO.0000000000000532>.
- [12] E.J. Mifsud, F.G. Hayden, A.C. Hurt, Antivirals targeting the polymerase complex of influenza viruses, *Antivir. Res.* 169 (2019) 104545–104554, <https://doi.org/10.1016/j.antiviral.2019.104545>.
- [13] Y. Furuta, B.B. Gowen, K. Takahashi, K. Shiraki, D.F. Smee, D.L. Barnard, Favipiravir (T-705), A novel viral RNA polymerase inhibitor, *Antivir. Res.* 100 (2013) 446–454, <https://doi.org/10.1016/j.antiviral.2013.09.015>.
- [14] T. Noshi, M. Kitano, K. Taniguchi, A. Yamamoto, S. Omoto, K. Baba, T. Hashimoto, K. Ishida, Y. Kushima, K. Hattori, M. Kawai, R. Yoshida, M. Kobayashi, T. Yoshinaga, A. Sato, M. Okamatsu, Y. Sakoda, H. Kida, T. Shishido, A. Naito, In vitro characterization of baloxavir acid, a first-in-class cap-dependent endonuclease inhibitor of the influenza virus polymerase PA subunit, *Antivir. Res.* 160 (2018) 109–117, <https://doi.org/10.1016/j.antiviral.2018.10.008>.
- [15] M.P. Clark, M.W. Ledebauer, I. Davies, R.A. Byrn, S.M. Jones, E. Perola, A. Tsai, M. Jacobs, K. Nti-Addae, U.K. Bandarage, M.J. Boyd, R.S. Bethiel, J.J. Court, H. Deng, J.P. Duffy, W.A. Dorsch, L.J. Farmer, H. Gao, W. Gu, K. Jackson, D.H. Jacobs, J.M. Kennedy, B. Ledford, J. Liang, F. Maltais, M. Murcko, T. Wang, M.W. Wannamaker, H.B. Bennett, J.R. Leeman, C. McNeil, W.P. Taylor, C. Memmott, M. Jiang, R. Rijnbrand, C. Bral, U. Germann, A. Nezami, Y. Zhang, F.G. Salituro, Y.L. Bennani, P.S. Charifon, Discovery of a novel, first-in-class, orally bioavailable azaindole inhibitor (VX-787) of influenza PB2, *J. Med. Chem.* 57 (2014) 6668–6678, <https://doi.org/10.1021/jm5007275>.
- [16] A. Loregian, B. Mercorelli, G. Nannetti, C. Compagnin, G. Palù, Antiviral strategies against influenza virus: towards new therapeutic approaches, *Cell. Mol. Life Sci.* 71 (2014) 3659–3683, <https://doi.org/10.1007/s001018-014-1615-2>.
- [17] J. Zhang, Y. Hu, R. Musharrafieh, H. Yin, J. Wang, Focusing on the influenza virus polymerase complex: recent progress in drug discovery and assay development, *Curr. Med. Chem.* 26 (2018) 2243–2263, <https://doi.org/10.2174/0929867325666180706112940>.
- [18] I. Giacchello, F. Musumeci, I. D'Agostino, C. Greco, G. Grossi, S. Schenone, Insights into RNA-dependent RNA polymerase inhibitors as anti-influenza virus agents, *Curr. Med. Chem.* 27 (2020) 1, <https://doi.org/10.2174/0929867327666200114115632>.
- [19] J.M. Wandzik, T. Kouba, S. Cusack, Structure and function of influenza polymerase, *Cold Spring Harb Perspect Med* 9 (2020) 38372–38391, <https://doi.org/10.1101/cshperspect.a038372>.
- [20] E. Fodor, A.J.W. te Velthuis, Structure and function of the influenza virus transcription and replication machinery, *Cold Spring Harb. Perspect. Med.* 9 (2019) 38398–38413, <https://doi.org/10.1101/cshperspect.a038398>.
- [21] X. He, J. Zhou, M. Bartlam, R. Zhang, J. Ma, Z. Lou, X. Li, J. Li, A. Joachimski, Z. Zeng, R. Ge, Z. Rao, Y. Liu, Crystal structure of the polymerase PAC–PB1N complex from an avian influenza H5N1 virus, *Nature* 454 (2008) 1123–1126, <https://doi.org/10.1038/nature07120>.
- [22] E. Obayashi, H. Yoshida, F. Kawai, N. Shibayama, A. Kawaguchi, K. Nagata, J.R.H. Tame, S.-Y. Park, The structural basis for an essential subunit interaction in influenza virus RNA polymerase, *Nature* 454 (2008) 1127–1131, <https://doi.org/10.1038/nature07225>.
- [23] G. Palù, A. Loregian, Inhibition of herpesvirus and influenza virus replication by blocking polymerase subunit interactions, *Antivir. Res.* 99 (2013) 318–327, <https://doi.org/10.1016/j.antiviral.2013.05.014>.
- [24] S. Massari, L. Goracci, J. Desantis, O. Tabarrini, Polymerase acidic protein–basic protein 1 (PA–PB1) protein–protein interaction as a target for next-generation anti-influenza therapeutics, *J. Med. Chem.* 59 (2016) 7699–7718, <https://doi.org/10.1021/acs.jmedchem.5b01474>.
- [25] S. Massari, J. Desantis, M.G. Nizi, V. Cecchetti, O. Tabarrini, Inhibition of influenza virus polymerase by interfering with its protein–protein interactions, *ACS Infect. Dis.* (2020), <https://doi.org/10.1021/acsinfectdis.0c00552>.
- [26] G. Muratore, B. Mercorelli, L. Goracci, G. Cruciani, P. Digard, G. Palù, A. Loregian, Human cytomegalovirus inhibitor AL18 also possesses activity against influenza A and B viruses, *Antimicrob. Agents Chemother.* 56 (2012) 6009–6013, <https://doi.org/10.1128/AAC.01219-12>.
- [27] G. Muratore, L. Goracci, B. Mercorelli, A. Foeglein, P. Digard, G. Cruciani, G. Palù, A. Loregian, Small molecule inhibitors of influenza A and B viruses that act by disrupting subunit interactions of the viral polymerase, *Proc. Natl. Acad. Sci. U.S.A.* 109 (2012) 6247–6252, <https://doi.org/10.1073/pnas.1119817109>.
- [28] I.M.L. Trist, G. Nannetti, C. Tintori, A.L. Fallacara, D. Deodato, B. Mercorelli, G. Palù, M. Wijtmans, T. Gospodova, E. Edink, M. Verheij, I. De Esch, L. Viteva, A. Loregian, M. Botta, 4,6-Diphenylpyridines as promising novel anti-influenza agents targeting the PA–PB1 protein–protein interaction: structure–activity relationships exploration with the aid of molecular modeling, *J. Med. Chem.* 59 (2016) 2688–2703, <https://doi.org/10.1021/acs.jmedchem.5b01935>.
- [29] S. Massari, G. Nannetti, L. Goracci, L. Sancineto, G. Muratore, S. Sabatini, G. Manfroni, B. Mercorelli, V. Cecchetti, M. Facchini, G. Palù, G. Cruciani, A. Loregian, O. Tabarrini, Structural investigation of cycloheptathiophene-3-carboxamide derivatives targeting influenza virus polymerase assembly, *J. Med. Chem.* 56 (2013) 10118–10131, <https://doi.org/10.1021/jm401560v>.
- [30] J. Desantis, G. Nannetti, S. Massari, M.L. Barreca, G. Manfroni, V. Cecchetti, G. Palù, L. Goracci, A. Loregian, O. Tabarrini, Exploring the cycloheptathiophene-3-carboxamide scaffold to disrupt the interactions of the influenza polymerase subunits and obtain potent anti-influenza activity, *Eur. J. Med. Chem.* 138 (2017) 128–139, <https://doi.org/10.1016/j.ejmech.2017.06.015>.
- [31] G. Nannetti, S. Massari, B. Mercorelli, C. Bertagnin, J. Desantis, G. Palù, O. Tabarrini, A. Loregian, Potent and broad-spectrum cycloheptathiophene-3-carboxamide compounds that target the PA–PB1 interaction of influenza virus RNA polymerase and possess a high barrier to drug resistance, *Antivir. Res.* 165 (2019) 55–64, <https://doi.org/10.1016/j.antiviral.2019.03.003>.
- [32] S. Massari, G. Nannetti, J. Desantis, G. Muratore, S. Sabatini, G. Manfroni, B. Mercorelli, V. Cecchetti, G. Palù, G. Cruciani, A. Loregian, L. Goracci, O. Tabarrini, A Broad anti-influenza hybrid small molecule that potently disrupts the interaction of polymerase acidic protein–basic protein 1 (PA–PB1) subunits, *J. Med. Chem.* 58 (2015) 3830–3842, <https://doi.org/10.1021/acs.jmedchem.5b00012>.
- [33] S. Lepri, G. Nannetti, G. Muratore, G. Cruciani, R. Ruzziconi, B. Mercorelli, G. Pal, A. Loregian, L. Goracci, Optimization of small-molecule inhibitors of influenza virus polymerase: from thiophene-3-carboxamide to polyamido scaffolds, *J. Med. Chem.* 57 (2014) 4337–4350, <https://doi.org/10.1021/jm500300r>.
- [34] I. D'Agostino, I. Giacchello, G. Nannetti, A.L. Fallacara, D. Deodato, F. Musumeci, G. Grossi, G. Palù, Y. Cau, I.M. Trist, A. Loregian, S. Schenone, M. Botta, Synthesis and biological evaluation of a library of hybrid derivatives as inhibitors of influenza virus PA–PB1 interaction, *Eur. J. Med. Chem.* 157 (2018) 743–758, <https://doi.org/10.1016/j.ejmech.2018.08.032>.
- [35] H. Liu, X. Yao, Molecular basis of the interaction for an essential subunit PA–PB1 in influenza virus RNA polymerase: insights from molecular dynamics simulation and free energy calculation, *Mol. Pharm.* 7 (2010) 75–85, <https://doi.org/10.1021/mp900131p>.
- [36] V.M. Chernyshev, A.V. Chernysheva, V.A. Taranushich, Synthesis of esters and amides of 5-amino-1,2,4-triazole-3-carboxylic and 5-amino-1,2,4-triazol-3-ylacetic acids, *Russ. J. Appl. Chem.* 79 (2006) 783–786, <https://doi.org/10.1134/S1070427206050168>.
- [37] S. Massari, J. Desantis, G. Nannetti, S. Sabatini, S. Tortorella, L. Goracci, V. Cecchetti, A. Loregian, O. Tabarrini, Efficient and regioselective one-step synthesis of 7-aryl-5-methyl- and 5-aryl-7-methyl-2-amino-[1,2,4]triazolo [1,5-a]pyrimidine derivatives, *Org. Biomol. Chem.* 15 (2017) 7944–7955, <https://doi.org/10.1039/C7OB02085F>.
- [38] E. Sopbué Fondjo, D. Döpp, G. Henkel, Reactions of some anellated 2-aminothiophenes with electron poor acetylenes, *Tetrahedron* 62 (2006) 7121–7131, <https://doi.org/10.1016/j.tet.2006.04.037>.
- [39] T. Masaoka, S. Chung, P. Caboni, J.W. Rausch, J.A. Wilson, H. Taskent-Sezgin, J.A. Beutler, G. Tocco, S.F.J. Le Grice, Exploiting drug-resistant enzymes as tools to identify thienopyrimidinone inhibitors of human immunodeficiency virus reverse transcriptase-associated ribonuclease H, *J. Med. Chem.* 56 (2013) 5436–5445, <https://doi.org/10.1021/jm400405z>.
- [40] K.P. Ravindranathan, V. Mandiyan, A.R. Ekkati, J.H. Bae, J. Schlessinger, W.L. Jorgensen, Discovery of novel fibroblast growth factor receptor 1 kinase inhibitors by structure-based virtual screening, *J. Med. Chem.* 53 (2010) 1662–1672, <https://doi.org/10.1021/jm901386e>.
- [41] V. Kogan, Preparation of Pyrido[3,4-B]indoles and Pyrimido[4,5-B]benzo[d]thiophen-4-Ones as Serotonergic and Dopaminergic Agents, 2008. WO2008/117269 A2.
- [42] T. Morwick, A. Berry, J. Brickwood, M. Cardozo, K. Catron, M. DeTuri, J. Emeigh, C. Homon, M. Hrapchak, S. Jacober, S. Jakes, P. Kaplita, T.A. Kelly, J. Ksiazek, M. Liuzzi, R. Magolda, C. Mao, D. Marshall, D. McNeil, A. Prokopowicz, C. Sarko, E. Scouten, C. Sledziona, S. Sun, J. Watrous, J.P. Wu, C.L. Cywin, Evolution of the thienopyrimidine class of inhibitors of IκB kinase-β: Part I: hit-to-lead strategies, *J. Med. Chem.* 49 (2006) 2898–2908, <https://doi.org/10.1021/jm0510979>.
- [43] K. Usui, K. Tanoue, K. Yamamoto, T. Shimizu, H. Suemune, Synthesis of substituted azulenes via Pt(II)-Catalyzed ring-expanding cycloisomerization, *Org. Lett.* 16 (2014) 4662–4665, <https://doi.org/10.1021/ol502270q>.
- [44] Y. Güneş, M.F. Polat, E. Sahin, F.F. Fleming, R. Altundas, Enantioselective synthesis of cyclic, quaternary oxonitriles, *J. Org. Chem.* 75 (2010) 7092–7098, <https://doi.org/10.1021/jo1011202>.
- [45] S. Massari, A. Corona, S. Distinto, J. Desantis, A. Credada, S. Sabatini, G. Manfroni, T. Felicetti, V. Cecchetti, C. Pannecouque, E. Maccioni, E. Tramontano, O. Tabarrini, From cycloheptathiophene-3-carboxamide to oxazinone-based derivatives as allosteric HIV-1 ribonuclease H inhibitors,

- J. Enzym. Inhib. Med. Chem. 34 (2019) 55–74, <https://doi.org/10.1080/14756366.2018.1523901>.
- [46] R. Romagnoli, P.G. Baraldi, M. Kimatrai Salvador, D. Preti, M. Aghazadeh Tabrizi, M. Bassetto, A. Brancale, E. Hamel, I. Castagliuolo, R. Bortolozzi, G. Basso, G. Viola, Synthesis and biological evaluation of 2-(alkoxycarbonyl)-3-anilinobenzo[b]thiophenes and thieno[2,3-b]pyridines as new potent anti-cancer agents, *J. Med. Chem.* 56 (2013) 2606–2618, <https://doi.org/10.1021/jm400043d>.
- [47] P. Leonczak, L.-J. Gao, A.T. Ramadori, E. Lescrinier, J. Rozenski, S. De Jonghe, P. Herdewijn, Synthesis and structure-activity relationship studies of 2-(1,3,4-oxadiazole-2(3H)-thione)-3-amino-5-arylthieno[2,3-b]pyridines as inhibitors of DRAK2, *ChemMedChem* 9 (2014) 2587–2601, <https://doi.org/10.1002/cmdc.201402234>.
- [48] T.D. Graneto, Matthew, Cathleen E. Hanau, Perry, Heteroaromatic Carboxamide Derivatives, Particularly 3-Aminothiophene-2-Carboxamides, Useful as Protein Kinase Inhibitors, for the Treatment of Cancer, Inflammation, and Inflammation-Related Disorders, 2003. WO03037886 (A2).
- [49] L.H. Klemm, J. Wang, L. Hawkins, Synthesis of 3-amino-2-carbamoylthiophene and its reaction with cycloalkanones to form imines, *J. Heterocycl. Chem.* 32 (1995) 1039–1041, <https://doi.org/10.1002/jhet.5570320361>.
- [50] B.E. Sleeb, A. Levit, I.P. Street, H. Falk, T. Hammonds, A.C. Wong, M.D. Charles, M.F. Olson, J.B. Baell, Identification of 3-aminothieno[2,3-b]pyridine-2-carboxamides and 4-aminobenzo[thieno[3,2-d]pyrimidines as LIMK1 inhibitors, *Medchemcomm* 2 (2011) 977–981, <https://doi.org/10.1039/c1md00137j>.
- [51] N.Y. Gorobets, B.H. Yousefi, F. Belaj, C.O.O. Kappe, Rapid microwave-assisted solution phase synthesis of substituted 2-pyridone libraries, *Tetrahedron* 60 (2004) 8633–8644, <https://doi.org/10.1016/j.tet.2004.05.100>.
- [52] M. F. Perrissin, D.C. Luu, G. Narcisse, F. Bakri-Logeais, Huguet, 4,5,6,7-Tetrahydrobenzo[b]- and 5,6,7,8-tetrahydro-4H-cyclohepta[b]thiophenes, *Eur. J. Med. Chem.* 15 (1980) 413–418.
- [53] Compounds 14 and 23 Were Previously Reported by Us in a Paper (Reference 14) Focused on the Development of Suitable Procedures for the Synthesis of the [1,2,4]-Triazolo[1,5-A]pyrimidine Nucleus.
- [54] C. Aldrich, C. Bertozzi, G.I. Georg, L. Kiessling, C. Lindsley, D. Liotta, K.M. Merz, A. Schepartz, S. Wang, The ecstasy and agony of assay interference compounds, *ACS Cent. Sci.* 3 (2017) 143–147, <https://doi.org/10.1021/acscentsci.7b00069>.
- [55] T. Sterling, J.J. Irwin, Zinc 15 – ligand discovery for everyone, *J. Chem. Inf. Model.* 55 (2015) 2324–2337, <https://doi.org/10.1021/acs.jcim.5b00559>.
- [56] A. Daina, O. Michielin, V. Zoete, SwissADME: a free web tool to evaluate pharmacokinetics, drug-likeness and medicinal chemistry friendliness of small molecules, *Sci. Rep.* 7 (2017) 1–13, <https://doi.org/10.1038/srep42717>.
- [57] C.A.S. Bergström, W.N. Charman, C.J.H. Porter, Computational prediction of formulation strategies for beyond-rule-of-5 compounds, *Adv. Drug Deliv. Rev.* 101 (2016) 6–21, <https://doi.org/10.1016/j.addr.2016.02.005>.
- [58] C.M. Wassvik, A.G. Holmén, R. Draheim, P. Artursson, C.A.S. Bergström, Molecular characteristics for solid-state limited solubility, *J. Med. Chem.* 51 (2008) 3035–3039, <https://doi.org/10.1021/jm701587d>.
- [59] C. Janiak, A critical account on  $\pi$ - $\pi$  stacking in metal complexes with aromatic nitrogen-containing ligands †, *J. Chem. Soc., Dalton Trans.* (2000) 3885–3896, <https://doi.org/10.1039/b003010o>.
- [60] B. Bonn, C. Leandersson, F. Fontaine, I. Zamora, Enhanced metabolite identification with MS<sup>E</sup> and a semi-automated software for structural elucidation, *Rapid Commun. Mass Spectrom.* 24 (2010) 3127–3138, <https://doi.org/10.1002/rcm.4753>.
- [61] I. Zamora, F. Fontaine, B. Serra, G. Plasencia, High-throughput, computer assisted, specific MetID. A revolution for drug discovery, *Drug Discov. Today Technol.* 10 (2013), <https://doi.org/10.1016/j.ddtec.2012.10.015> e199–e205.
- [62] A. Brink, F. Fontaine, M. Marschmann, B. Steinhuber, E.N. Cece, I. Zamora, A. Pähler, Post-acquisition analysis of untargeted accurate mass quadrupole time-of-flight MS<sup>E</sup> data for multiple collision-induced neutral losses and fragment ions of glutathione conjugates, *Rapid Commun. Mass Spectrom.* 28 (2014) 2695–2703, <https://doi.org/10.1002/rcm.7062>.
- [63] T. Radchenko, F. Fontaine, L. Moretoni, I. Zamora, WebMetabase: cleavage sites analysis tool for natural and unnatural substrates from diverse data source, *Bioinformatics* 35 (2019) 650–655, <https://doi.org/10.1093/bioinformatics/bty667>.
- [64] G. Cruciani, E. Carosati, B. De Boeck, K. Ethirajulu, C. Mackie, T. Howe, R. Vianello, MetaSite: understanding metabolism in human cytochromes from the perspective of the chemist, *J. Med. Chem.* 48 (2005) 6970–6979, <https://doi.org/10.1021/jm050529c>.
- [65] M. Baroni, G. Cruciani, S. Sciabola, F. Perruccio, J.S. Mason, A common reference framework for analyzing/comparing proteins and ligands. Fingerprints for Ligands and Proteins (FLAP): theory and application, *J. Chem. Inf. Model.* 47 (2007) 279–294, <https://doi.org/10.1021/ci600253e>.
- [66] T. Masaoka, S. Chung, P. Caboni, J.W. Rausch, J.A. Wilson, H. Taskent-Sezgin, J.A. Beutler, G. Tocco, S.F.J. Le Grice, Exploiting drug-resistant enzymes as tools to identify thienopyrimidinone inhibitors of human immunodeficiency virus reverse transcriptase-associated ribonuclease H, *J. Med. Chem.* 56 (2013) 5436–5445, <https://doi.org/10.1021/jm400405z>.
- [67] G. Cruciani, F. Milletti, L. Storchi, G. Sforza, L. Goracci, *In silico* pK<sub>a</sub> prediction and ADME profiling, *Chem. Biodivers.* 6 (2009) 1812–1821, <https://doi.org/10.1002/cbdv.200900153>.
- [68] S. Fawell, J. Seery, Y. Daikh, C. Moore, L.L. Chen, B. Pepinsky, J. Barsoum, Tat-mediated delivery of heterologous proteins into cells, *Proc. Natl. Acad. Sci. U.S.A.* 91 (1994) 664–668.
- [69] A. Loregian, B.A. Appleton, J.M. Hogle, D.M. Coen, Residues of human cytomegalovirus DNA polymerase catalytic subunit UL54 that are necessary and sufficient for interaction with the accessory protein UL44, *J. Virol.* 78 (2004) 158–167, <https://doi.org/10.1128/jvi.78.1.158-167.2004>.
- [70] A. Loregian, D.M. Coen, Selective anti-cytomegalovirus compounds discovered by screening for inhibitors of subunit interactions of the viral polymerase, *Chem. Biol.* 13 (2006) 191–200, <https://doi.org/10.1016/j.chembiol.2005.12.002>.
- [71] K.A. Dehring, H.L. Workman, K.D. Miller, A. Mandagere, S.K. Poole, Automated robotic liquid handling/laser-based nephelometry system for high throughput measurement of kinetic aqueous solubility, *J. Pharmaceut. Biomed. Anal.* 36 (2004) 447–456, <https://doi.org/10.1016/j.jpba.2004.07.022>.